Proton and Ion Linear Accelerators

7. Radio Frequency Quadrupole (RFQ) Accelerator

Yuri Batygin
Los Alamos National Laboratory

U.S. Particle Accelerator School

June 7 - July 2, 2021

Short History of RFQ

1956 V.V. Vladimirsky proposed the idea of RFQ focusing

4 electrodes with RF voltage have been used for mass separation since 1950s

1962 V.A.Teplyakov and independently P.Lapostolle proposed drift tube linac with rectangular apertures

1969 I.M. Kapchinski and V.A. Teplyakov invented RFQ. The first publication in 1969 in the Proc. of HEP Accelerator Conference

1972 First operational RFQ in Protvino, Russia; Proton beam accelerated from 100 keV to 600 keV

1980- RFQ is tested in LANL: 30 mA beam accelerated from 100 keV to 650 keV

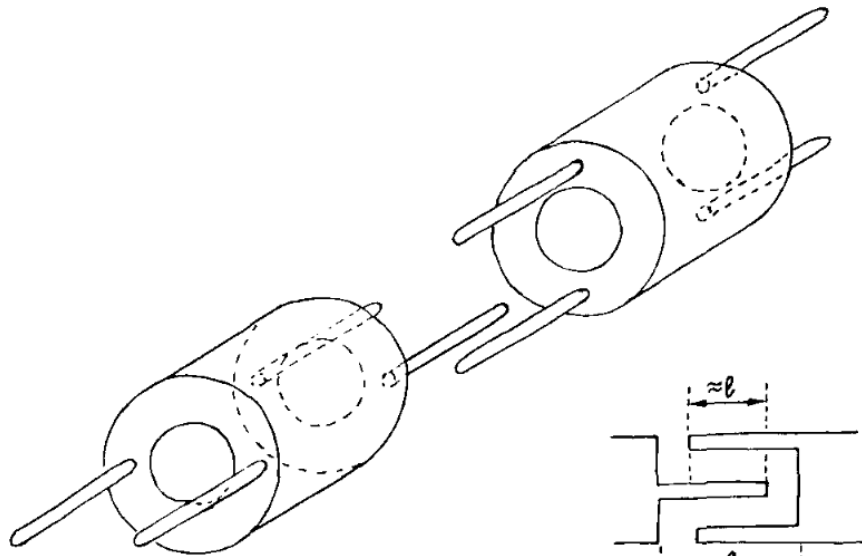# RFQ Focusing in Spatially Periodic Structures

FIG. 1

V.V.Vladimirsky's idea was to skip axial-symmetry of electric field in accelerating gaps. Drift tubes with fingers inserted into accelerating gaps were proposed The azimuthat orientation of the fingers periodically changed by 90º.
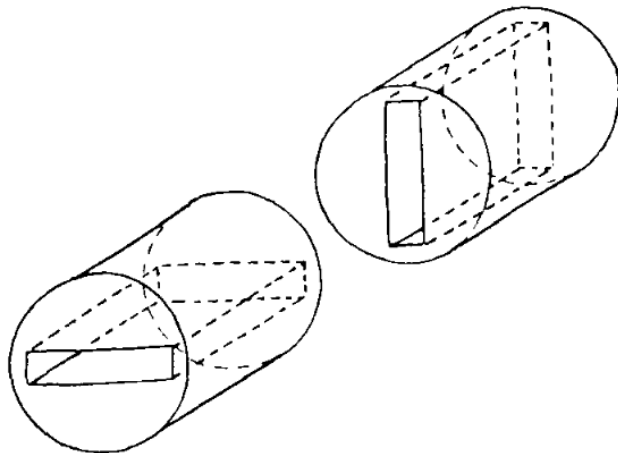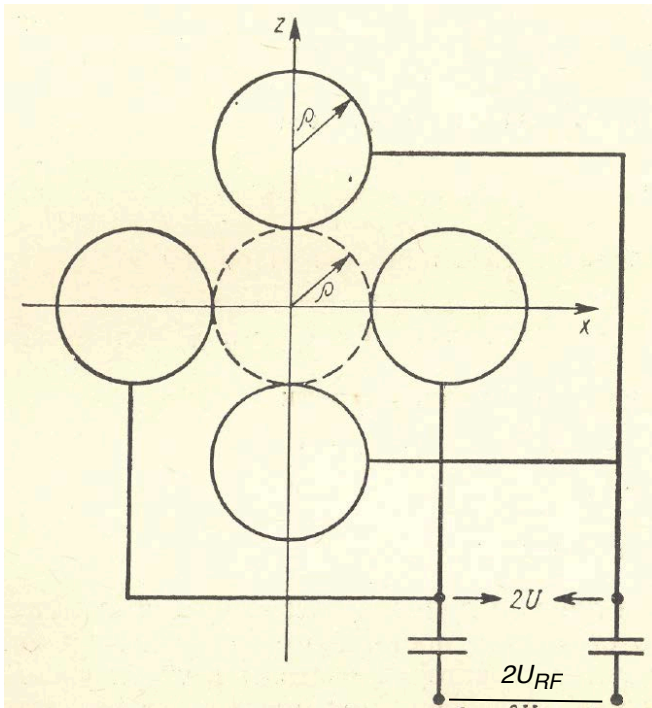

FIG. 2

In 1962 V.A.Teplyakov and independently P.Lapostolle proposed drift tube linac with rectangular apertures.

Los Alamos
NATIONAL LABORATORY
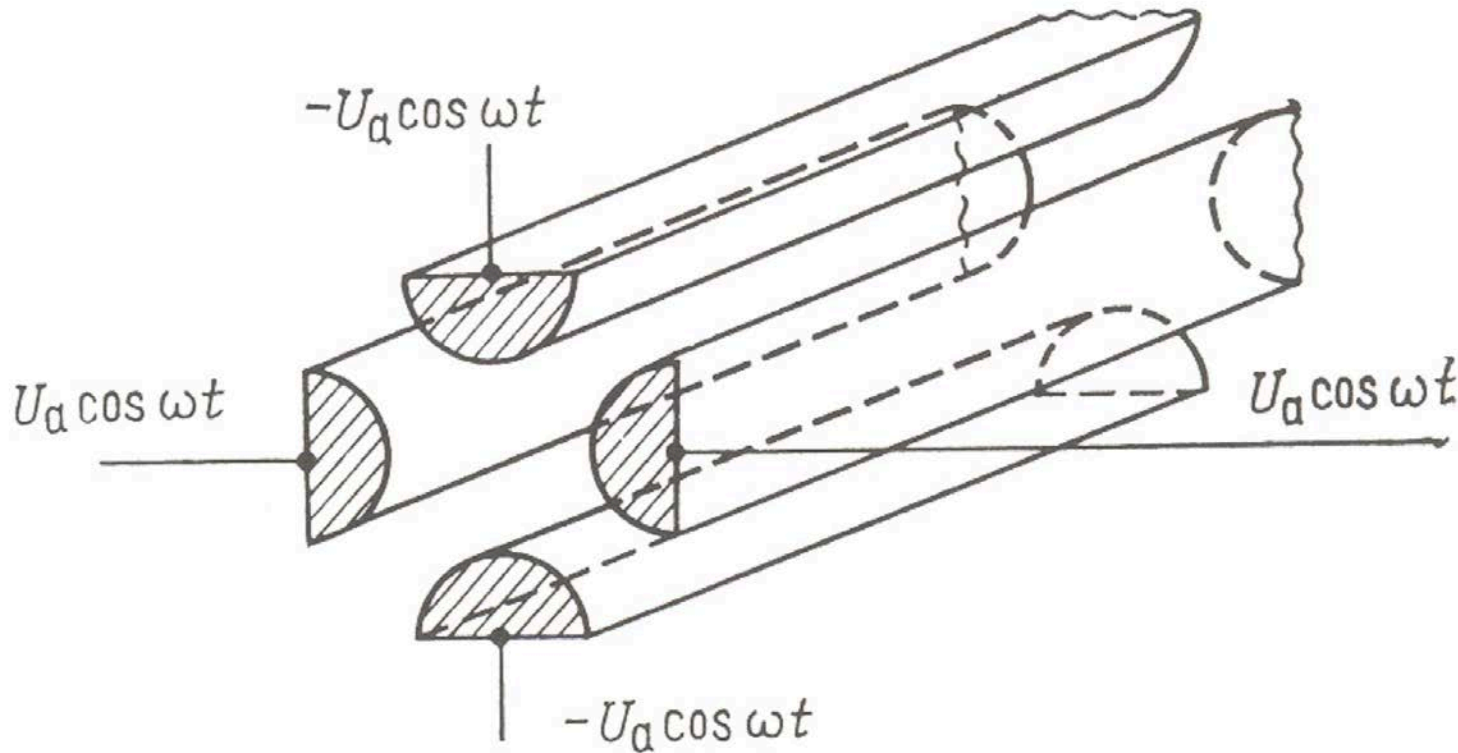
Radio Frequency Separator (Paul Trap)

The quadrupole consists of four parallel metal rods. Each opposing rod pair is connected together electrically, and a (RF) voltage with a DC offset voltage is applied between one pair of rods and the other. Ions travel down the quadrupole between the rods. Only ions of a certain mass-to-charge ratio will reach the detector for a given ratio of voltages: other ions have unstable trajectories and will collide with the rods. This permits selection of an ion with a particular *A/Z* or allows the operator to scan for a range of *A/Z*-values by continuously varying the applied voltage.

Bunch of ions

Los Alamos
NATIONAL LABORATORY
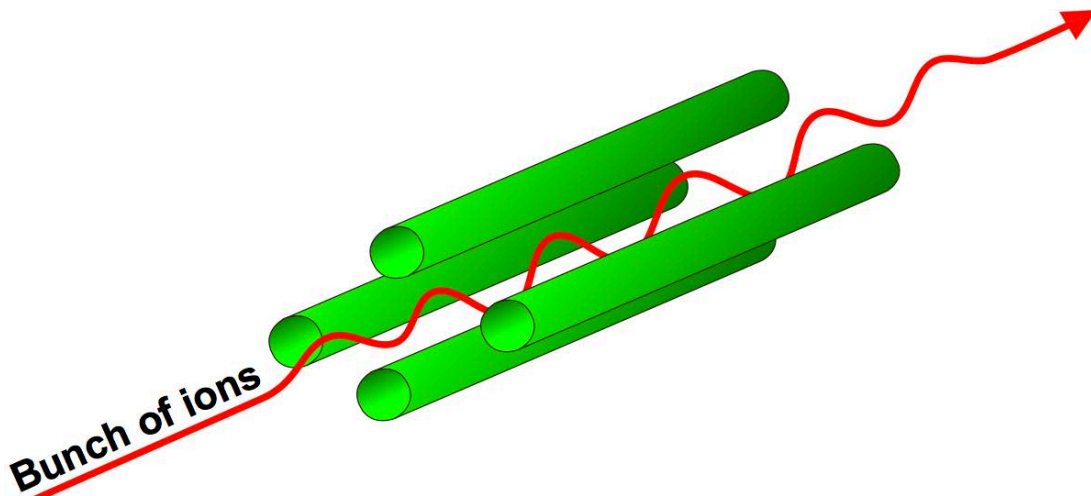
Radio Frequency Quadrupole

$-U_a \cos \omega t$

$U_a \cos \omega t$

$U_a \cos \omega t$

$-U_a \cos \omega t$

$$U(r,\theta,t) = U_a \left(\frac{r}{a} \right)^2 \cos(2\theta)\cos(\omega t)$$

Potential between electrodes $U_L = 2U_a$

Los Alamos
NATIONAL LABORATORY

Dynamics in 4-Rods Uniform Structure

Equations of transverse oscillations in 4-rods uniform focusing structure

$$m\frac{d^2x}{dt^2} = -\frac{2qU_a x}{a^2}\cos\omega t$$

$$m\frac{d^2y}{dt^2} = \frac{2qU_a x}{a^2}\cos\omega t$$

Averaging method

$$f_1 = \frac{2qU_a x}{a^2} \qquad \omega = \frac{2\pi c}{\lambda}$$

$$\xi = -\frac{f_1}{m\omega^2}$$

Equation of averaged oscillations in 4-rods structure

$$\frac{d^2X}{dt^2} + \Omega_r^2 X = 0$$

Frequency of averaged oscillations in 4-rods structure

$$\boxed{\Omega_r = \frac{\sqrt{2}qU_a\lambda}{2\pi mca^2}}$$

Small oscillation term

$$\boxed{\upsilon_{max} = \frac{|\xi_{max}|}{x} = \frac{1}{2\pi^2}\frac{qU_a}{mc^2}\frac{\lambda^2}{a^2}}$$

Los Alamos
NATIONAL LABORATORY

Axial Accelerating Field

To produce the axial field suppose we modulate the vane tips along the axial direction.

If this is done with x and y modulations that are 180 degrees out of phase, the on-axis potential will follow the potential variations of the vane tips and a sinusoidal on-axis electric field is produced.
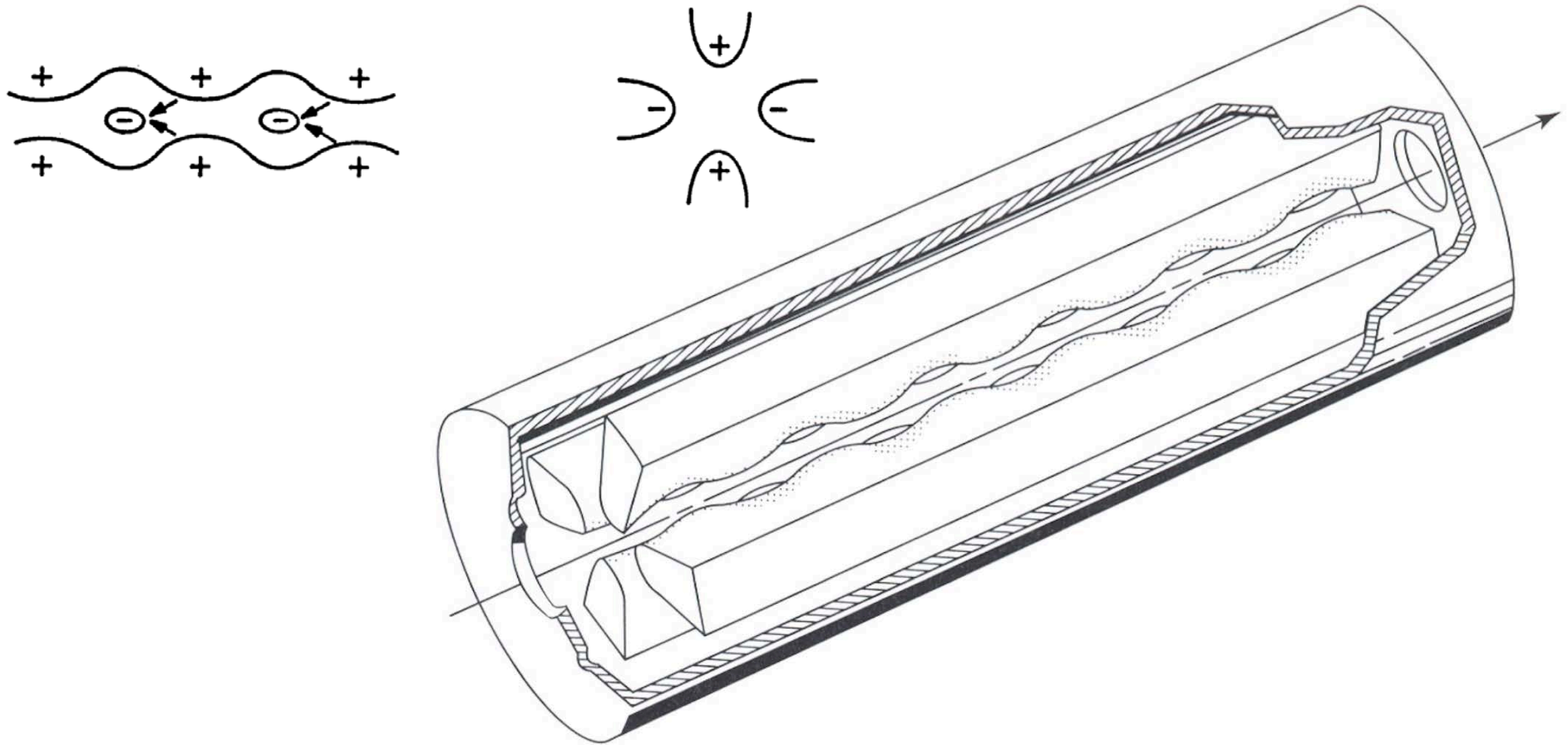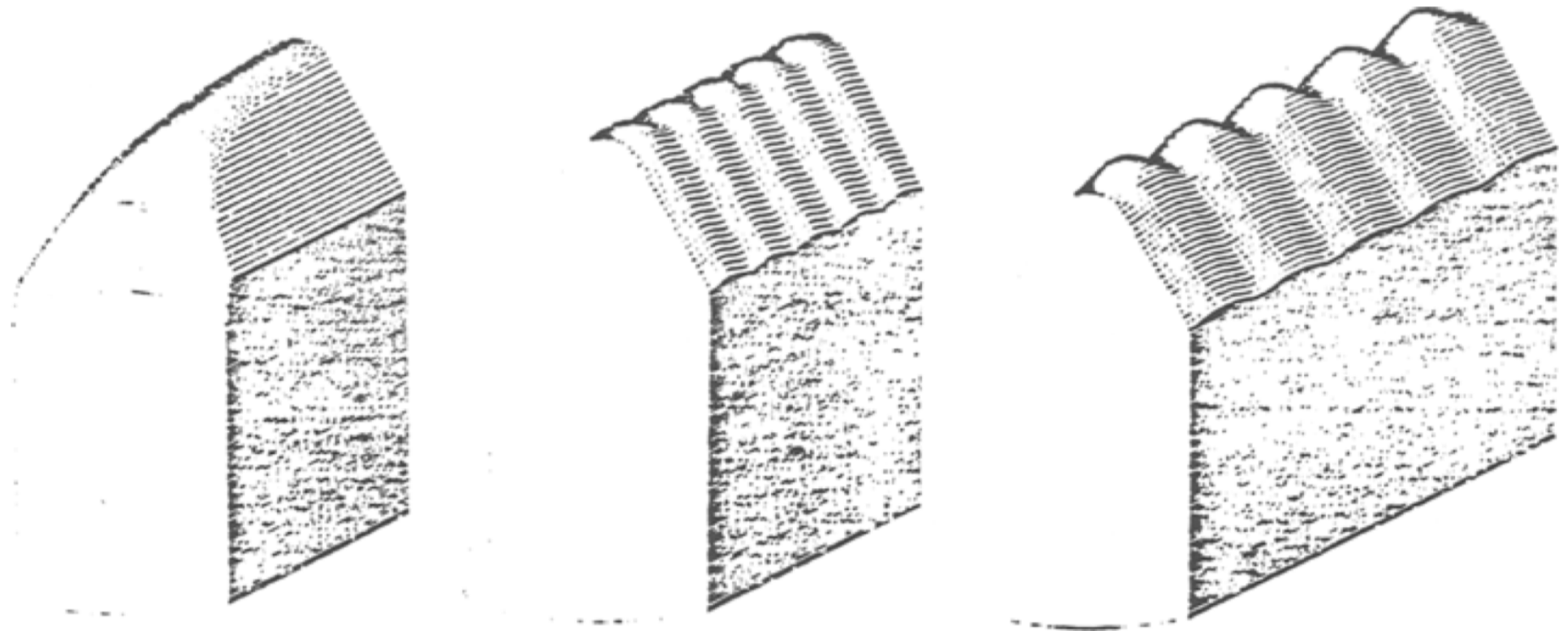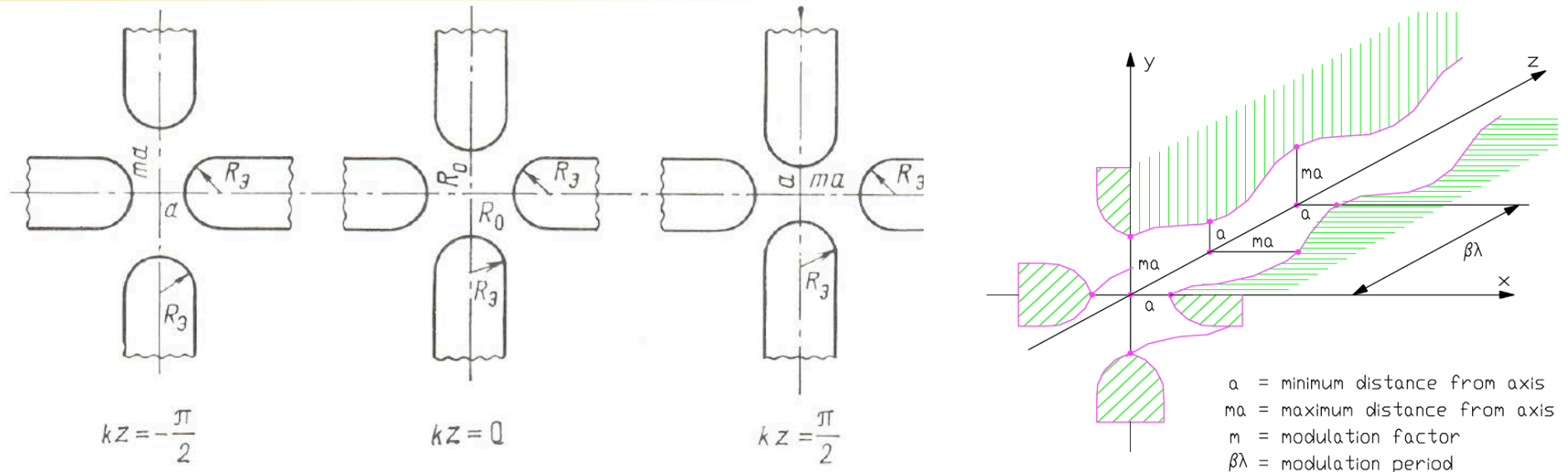
Modulated RFQ Electrodes

Figure 6: Scalloped Vane Tips   (J. Staples, 1992)

Potential of RFQ Structure

Cross sections of modulated electrodes in the RFQ accelerating structure.

RFQ potential of this structure is a solution of Laplace's equation in 3D domain:

$$\frac{\partial^2 V}{\partial r^2} + \frac{1}{r}\frac{\partial V}{\partial r} + \frac{1}{r^2}\frac{\partial^2 V}{\partial \theta^2} + \frac{\partial^2 V}{\partial z^2} = 0$$

Boundary conditions:

$V(r,\theta,z) = V(r,-\theta,z)$

$V(r,\theta,z) = V(r,\theta,-z)$

$V(r,\theta,z) = V(r,\theta+\pi,z)$

$V(r,\theta,z) = -V(r,\theta+\frac{\pi}{2},z+\frac{L}{2})$

$$V(r,\theta,z) = \sum_{s=0}^{\infty} A_s r^{2(2s+1)}\cos[2(2s+1)\theta]$$
$$+\sum_{n=1}^{\infty}\sum_{s=0}^{\infty} A_{ns} I_{2s}(k_z n r)\cos(2s\theta)\sin(k_z n z)$$

Los Alamos
NATIONAL LABORATORY

Equation for Ideal Electrodes

Potential containing first two terms in potential expansion

$$V(r,\theta,z) = -U_a[\chi(\frac{r}{a})^2 \cos 2\theta + \frac{4T}{\pi} I_o(\frac{2\pi r}{\beta\lambda})\sin(\frac{2\pi z}{\beta\lambda})]$$

Equation for ideal electrode surface:

$$r^2 \cos 2\theta = (\frac{a^2}{\chi})[\pm 1 - \frac{4T}{\pi} I_o(\frac{2\pi r}{\beta\lambda})\sin(\frac{2\pi z}{\beta\lambda})]$$

Shape of ideal electrodes depend on position z. At z=0 electrodes have pure hyperbolic shape.
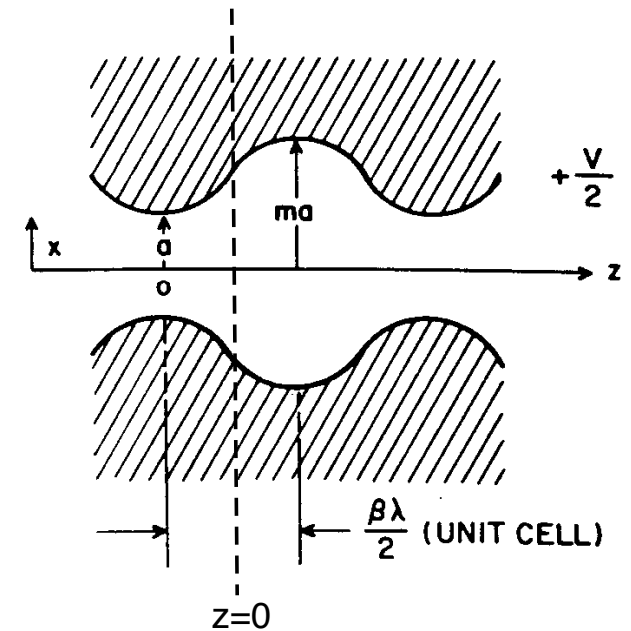
From boundary conditions determine coefficients T, χ

$$V(r,\theta,z) = U_a$$

$$r = a, \theta = 0, z = \frac{\beta\lambda}{4}$$

$$r = ma, \theta = 0, z = \frac{3\beta\lambda}{4}$$

$$T = \frac{\pi}{4} \frac{m^2 - 1}{m^2 I_o(\frac{2\pi a}{\beta\lambda}) + I_o(\frac{2m\pi a}{\beta\lambda})}$$

$$\chi = 1 - \frac{4T}{\pi} I_o(\frac{2\pi a}{\beta\lambda})$$

Common notation: efficiency of acceleration

$$A = \frac{4}{\pi} T$$

Ideal RFQ Electrodes and Energy Gain per Cell

Radius of electrodes at the point of exact quadrupole symmetry
$$R_o = \frac{a + ma}{2}$$
$$\boxed{R_o = \frac{a}{\sqrt{\chi}}}$$

Aperture of the channel
$$a = R_o \frac{2}{m+1}$$

Equations for electrode modulation

$$x = R_o[1 + \frac{m-1}{m+1}\sin(\frac{2\pi z}{\beta\lambda})]$$
$$y = R_o[1 - \frac{m-1}{m+1}\sin(\frac{2\pi z}{\beta\lambda})]$$

Longitudinal field component
$$E_z(r,z,t) = 4\frac{U_L T}{\beta\lambda} I_o(\frac{2\pi r}{\beta\lambda})\cos(\frac{2\pi z}{\beta\lambda})\cos(\omega t)$$

Equivalent traveling wave
$$E = 2\frac{U_L T}{\beta\lambda} I_o(\frac{2\pi r}{\beta\lambda})\cos\varphi$$

Energy gain per RFQ cell $\beta\lambda/2$
$$\boxed{\Delta W = qU_L T \cos\varphi}$$

Los Alamos
NATIONAL LABORATORY

Vane Tip Machining

Transverse radius of curvature of electrodes is usually selected to be 70% to 100% of Ro.
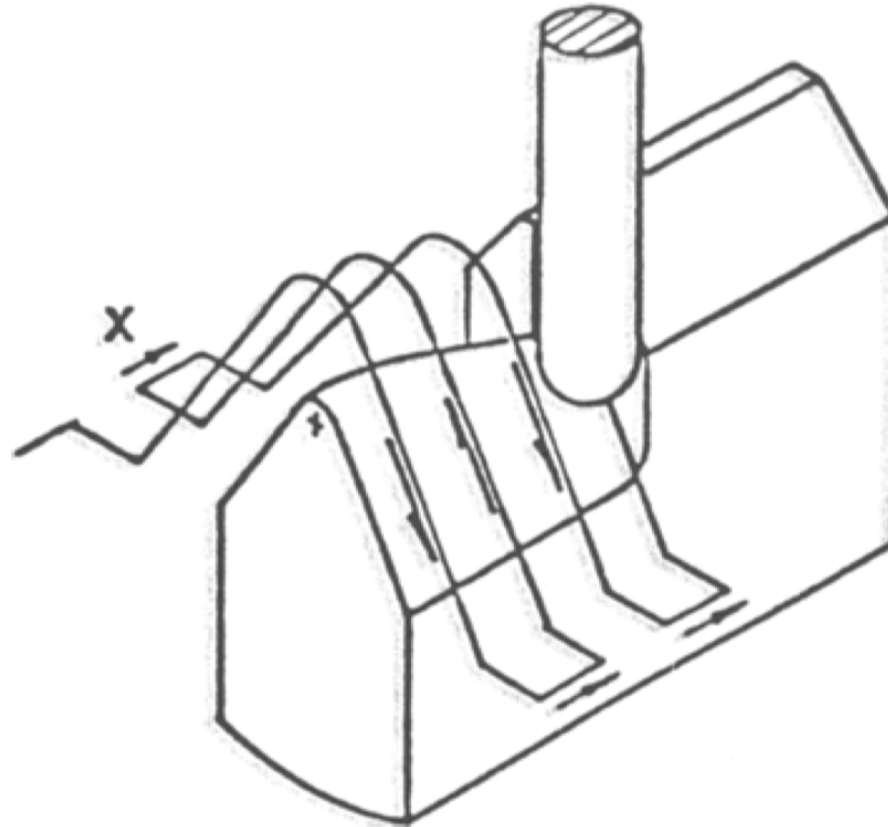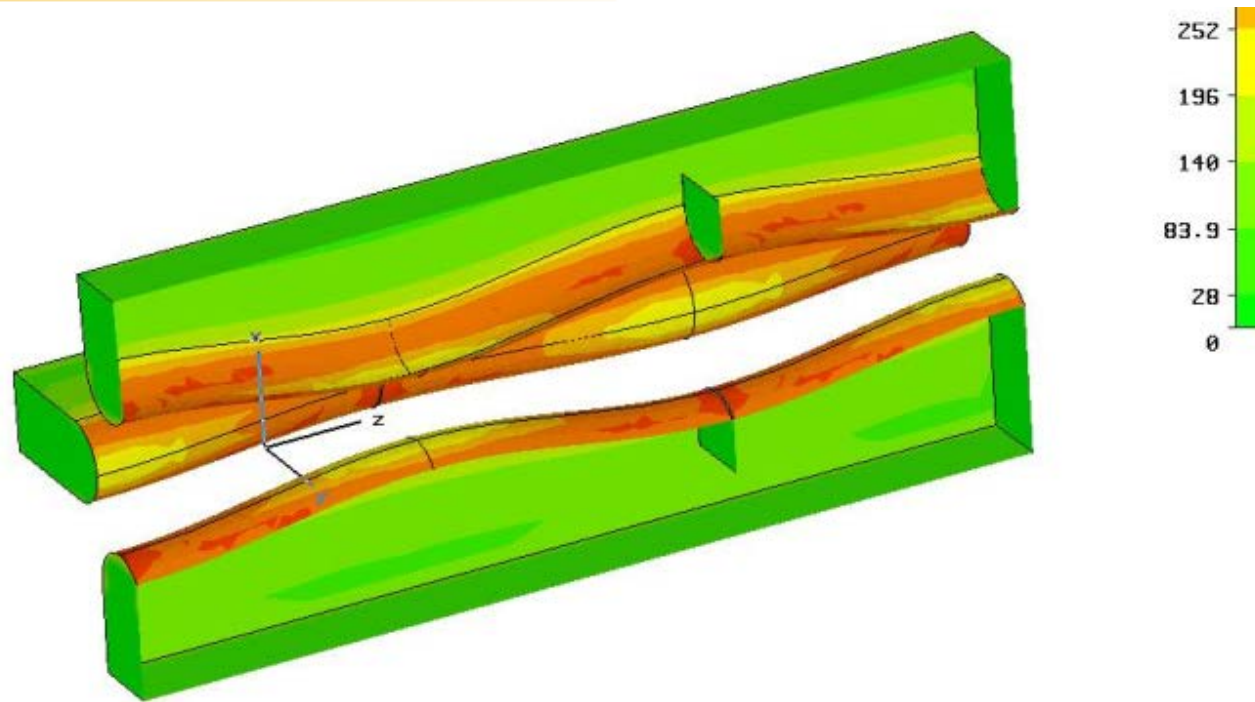

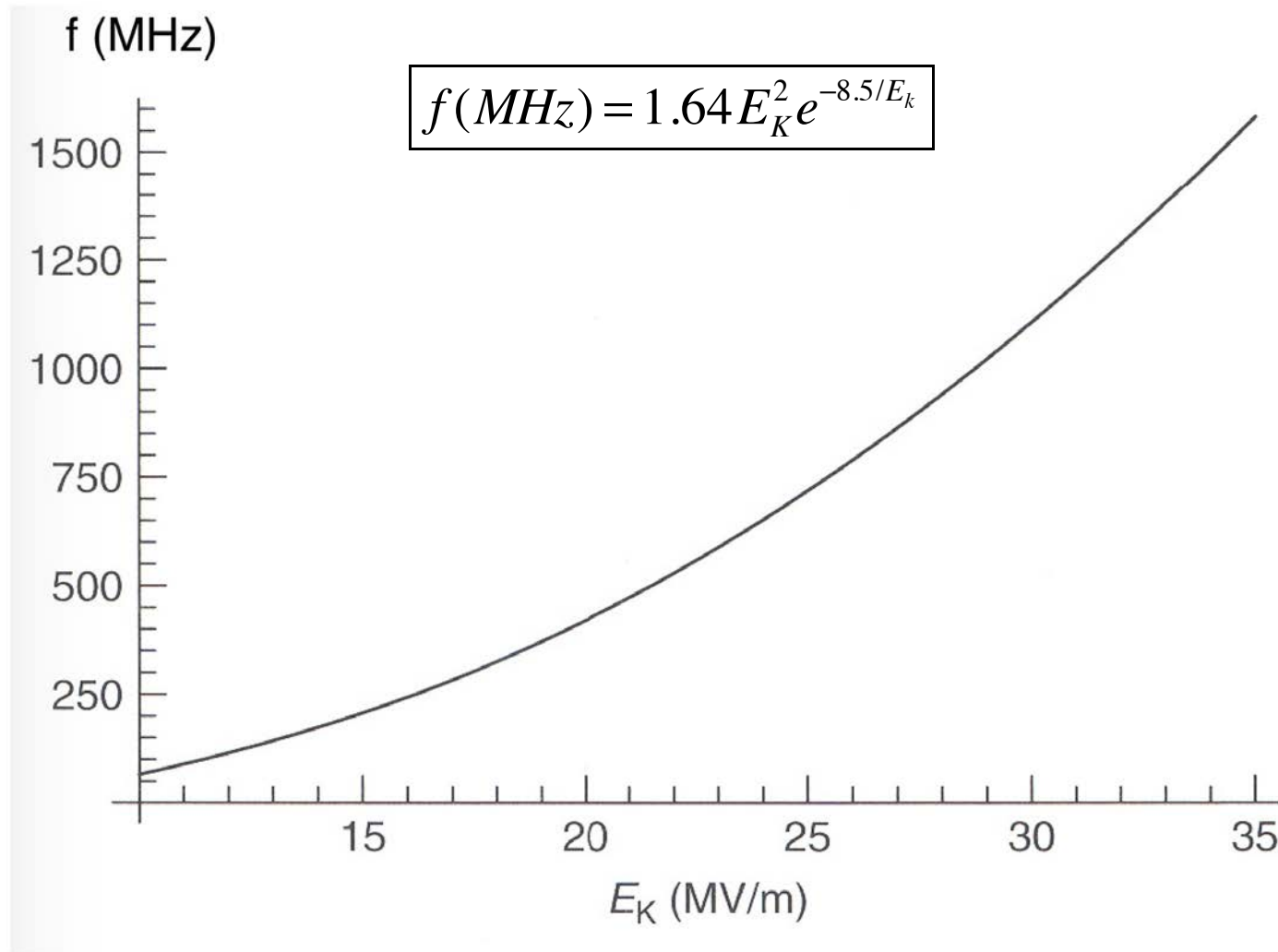Figure 11: Tool path to cut variable curvature vane tip.

Peak Field

Field distribution at RFQ electrodes (P. Ostroumov, 2006)

Maximal RFQ field is achieved at the surface of electrode where *r = ma* *(I.Kapchinsky, 1972))*

$$E_{max} = \frac{U_L}{a}[\chi m + 4T(\frac{a}{\beta\lambda})I_1(\frac{2\pi ma}{\beta\lambda})]$$

Usually peak surface field is held below $2E_k$ (Kilpatrick limit).
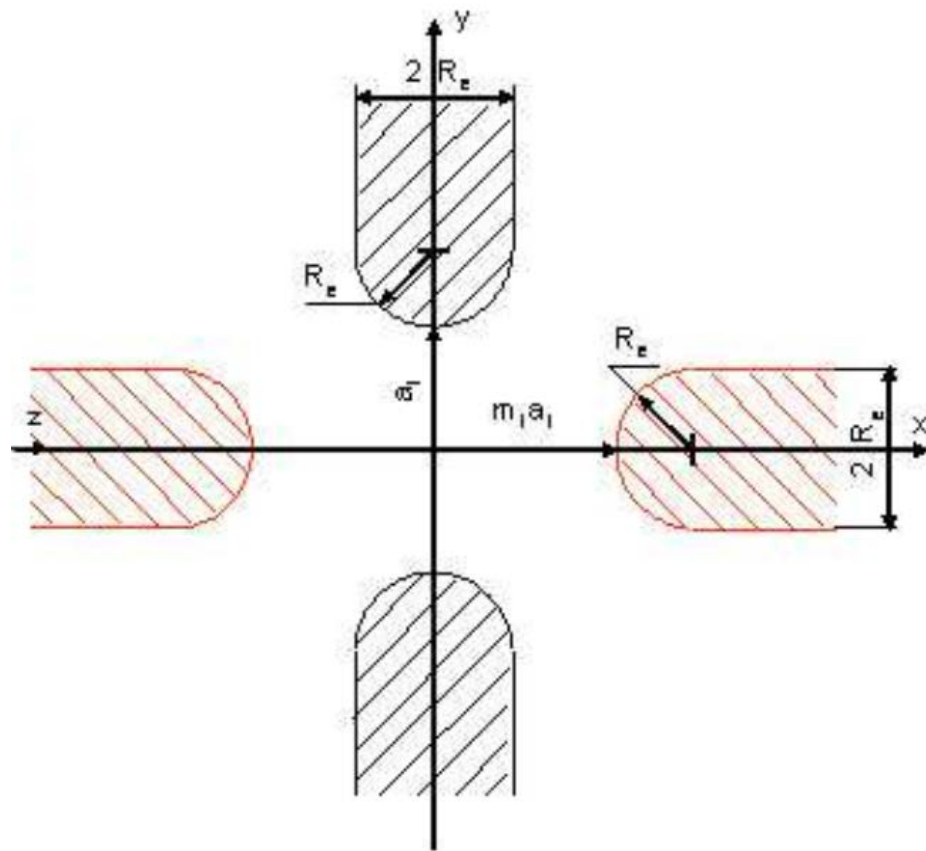
Kilpatrick Limited RF Field

$$f(MHz) = 1.64 E_K^2 e^{-8.5/E_k}$$

Kilpatrick limited RF field E_k [MV/m]

Modified Kilpatrick Limit for RFQ

Modified Kilpatrick limit for RFQ
(A.A. Kolomiets, 2005):

$$gE_{KP}^3\left(1-\exp\left(\frac{-48.6E_{KP}}{gf^2}\right)\right)=1.8\cdot 10^5\exp\left(\frac{170}{E_{KP}}\right)$$

$$g=R_0\left(\sqrt{2}\left(1+\frac{R_e}{R_0}\right)-2\frac{R_e}{R_0}\right)$$

E_{KP} [kV/cm] is the Kilpatrick limit of the peak surface field

f [MHz] is the operational frequency

g[cm] is the minimum distance between unmodulated RFQ electrodes

$$R_o=\frac{a}{\sqrt{\chi}}$$ is the average radius

Hamiltonian of Particle Motion in RFQ Field

Hamiltonian of particle motion in RFQ field

$$H = \frac{p_x^2 + p_y^2 + p_z^2}{2m} - qU_a[\chi(\frac{r}{a})^2 \cos 2\theta + \frac{4T}{\pi} I_o(\frac{2\pi r}{\beta\lambda})\sin(\frac{2\pi z}{\beta\lambda})]\cos\omega t$$

Longitudinal momentum deviation from synchronous particle

$$p_\zeta = p_z - p_s$$

Deviation from synchronous particle

$$\zeta = z - z_s$$

Hamiltonian in new variables:

$$H = \frac{p_x^2 + p_y^2 + p_\xi^2}{2m} - qU_a\chi(\frac{r}{a})^2 \cos 2\theta \cos\omega t + qU_a\frac{2T}{\pi}[I_o(\frac{2\pi r}{\beta\lambda})\sin(\varphi_s - k_z\xi) + k_z\xi\cos\varphi_s]$$

Hamiltonian of Averaged Particle Oscillations

After averaging $\quad \dfrac{2qU_a\chi}{ma^2}\cos\omega t \rightarrow \Omega_r^2$, Hamiltonian of averaged particle motion

$$H = \frac{p_x^2 + p_y^2 + p_\xi^2}{2m} + \frac{m\Omega_r^2 r^2}{2} + qU_a\frac{2T}{\pi}[I_o(\frac{2\pi r}{\beta\lambda})\sin(\varphi_s - k_z\xi) + k_z\xi\cos\varphi_s]$$

Transverse oscillation frequency

$$\Omega_r = \frac{\omega}{\sqrt{2}\pi^2}\chi\frac{qU_L}{mc^2}(\frac{\lambda}{2a})^2$$

Hamiltonian of longitudinal motion:

$$H = \frac{p_\xi^2}{2m} + \frac{qU_L T}{\pi}[I_o(\frac{2\pi r}{\beta\lambda})\sin(\varphi_s - k_z\xi) + k_z\xi\cos\varphi_s]$$

For small longitudinal oscillations

$$H = \frac{p_\xi^2}{2m} + m\Omega^2 I_o(k_z r)\frac{\zeta^2}{2} + m\Omega^2\frac{\zeta}{k_z\, tg\varphi_s}[I_o(k_z r) - 1]$$

Longitudinal oscillation frequency is determined by

$$\Omega^2 = \omega^2\frac{qU_L T\sin\varphi_s}{\pi m(\beta c)^2}$$

In RFQ accelerator longitudinal oscillations depend on transverse oscillations.

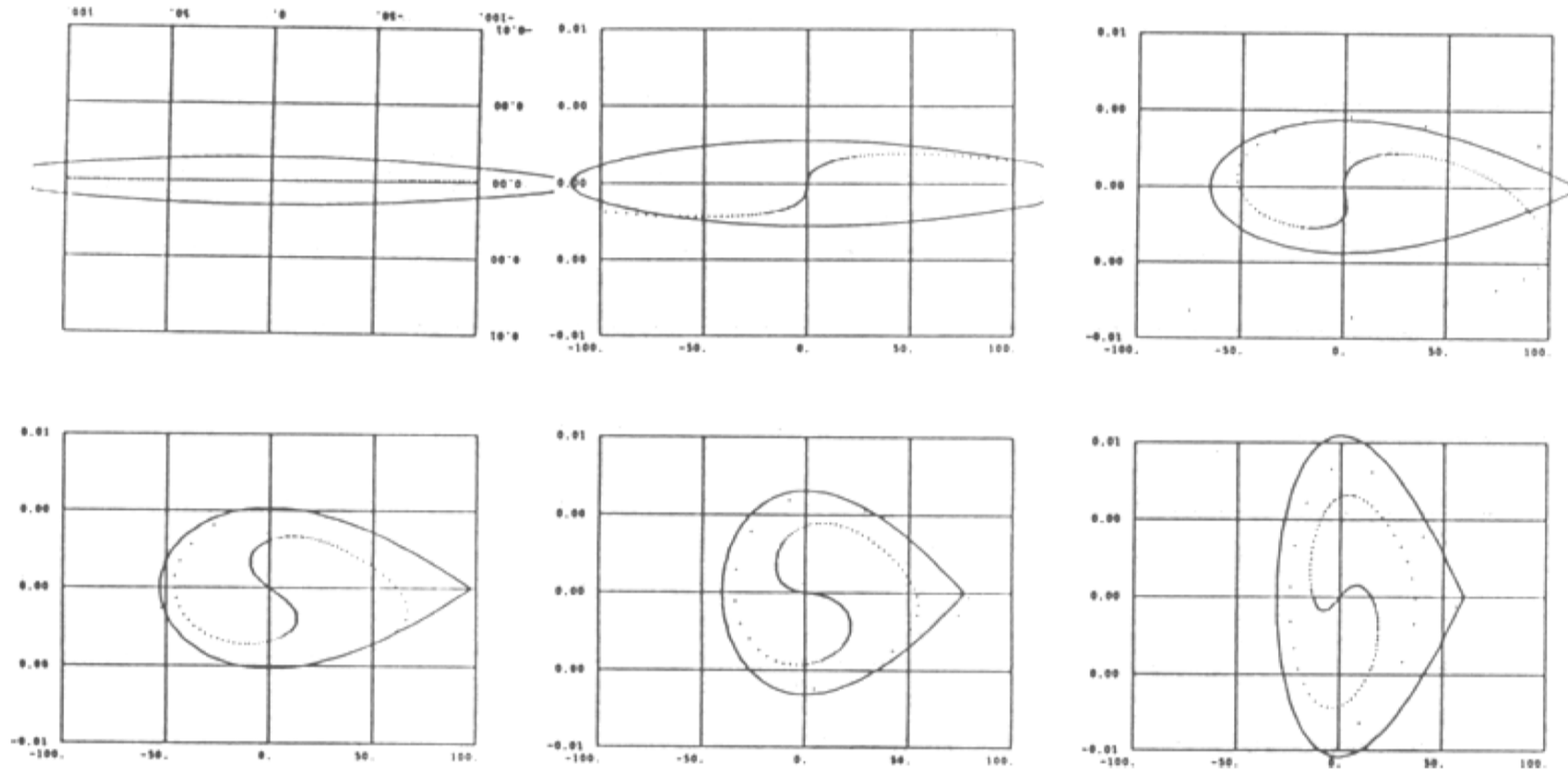**Los Alamos** NATIONAL LABORATORY

Figure 8: Adiabatically Bunching Longitudinal Phase Space

Quasi-Stationary Bunching in RFQ

Basic idea of quasi-stationary bunching is to keep geometrical bunch size and longitudinal beam phase space distribution constant. In this case, bunches do not oscillate and space charge density is close to constant. Bunches are cut from continuous beam and move apart from each other without changes in beam distribution.

Geometrical length of separatrix is

$$Z_s = \beta\lambda\frac{\Phi_s}{2\pi}$$

To keep length of the bunch, we impose condition Z_s = const

$$\boxed{\beta\,\Phi_s = const}$$

Separatrix is related to synchronous phase through condition

$$tg\left|\varphi_s\right| = \frac{\Phi_s - \sin\Phi_s}{1 - \cos\Phi_s}$$

Synchronous phase has to decrease from φ_s = -90° till final value φ_{fin} to keep product $\beta\Phi_s$ = const.

Los Alamos
NATIONAL LABORATORY

Quasi-Stationary Bunching in RFQ (cont.)

Hamiltonian of small longitudinal oscillations near axis

$$H = \frac{p_\xi^2}{2m} + m\Omega^2 \frac{\zeta^2}{2}$$

Equation for phase space trajectory

$$\frac{p_\zeta^2}{p_{\zeta\,max}^2} + \frac{\zeta^2}{\zeta_{max}^2} = 1$$

Semi-axis of ellipse

$$\zeta_{max} = \frac{1}{\Omega}\sqrt{\frac{2H}{m}} \qquad p_{\zeta\,max} = \sqrt{2Hm} = \zeta_{max}\Omega m$$

According to adiabatic theorem, phase space area is constant:

$$\boxed{\varepsilon_z = \frac{p_{\zeta\,max}}{mc}\zeta_{max} = \zeta_{max}^2 \frac{\Omega}{c}}$$

Condition $\Omega = const$ guarantees conservation of phase space trajectories and preserves distribution of charge density within linear part of separatrix.

$$\boxed{\frac{TU_L \sin\varphi_s}{\beta_s^2} = const}$$

Los Alamos
NATIONAL LABORATORY

Design of Quasi-Stationary Buncher

Conditions Ω = const , Z_s = const determine dependence of acceleration efficiency T and synchronous phase φ_s on energy of synchronous particle W_s

$$\Phi_s(\varphi_s) = \Phi_s(\varphi_{fin})\sqrt{\frac{W_{fin}}{W_s}}$$

$$T(W_s) = T(W_{fin})\frac{W_s \sin\varphi_{fin}}{W_{fin} \sin\varphi_s}$$

Synchronous phase is related to separatrix as

$$tg|\varphi_s| = \frac{\Phi_s - \sin\Phi_s}{1 - \cos\Phi_s}$$

Design starts with determination of initial values of φ_s , W_s , and final buncher values of φ_{fin} , W_{fin}. At every iterative step the new value of energy of synchronous particle is determined:

$$\Delta W_s = qU_L T \cos\varphi_s$$

which determines new values of synchronous phase φ_s and new value of acceleration efficiency T. The value of T and W_s determine modulation coefficient and cell length.
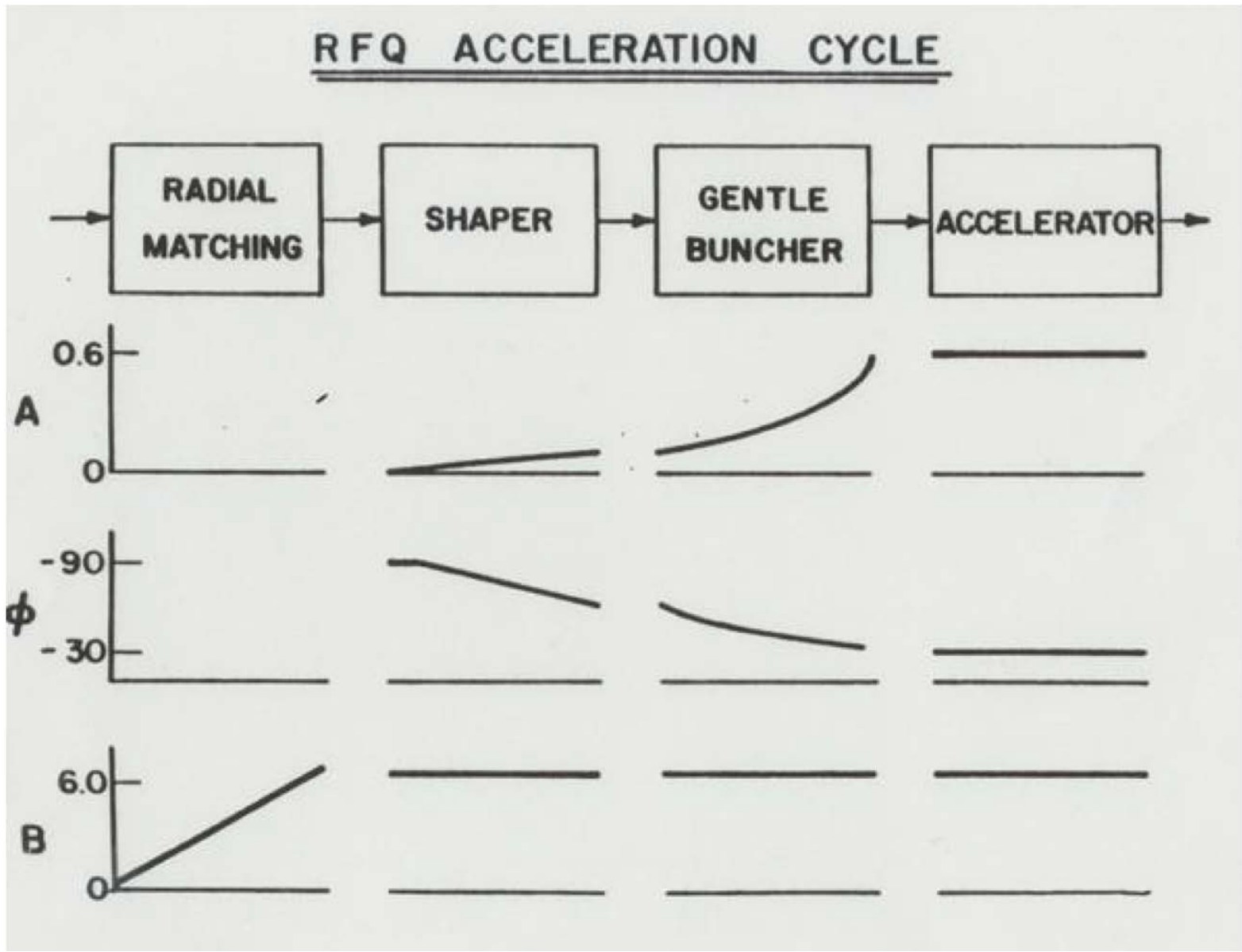
Los Alamos
NATIONAL LABORATORY
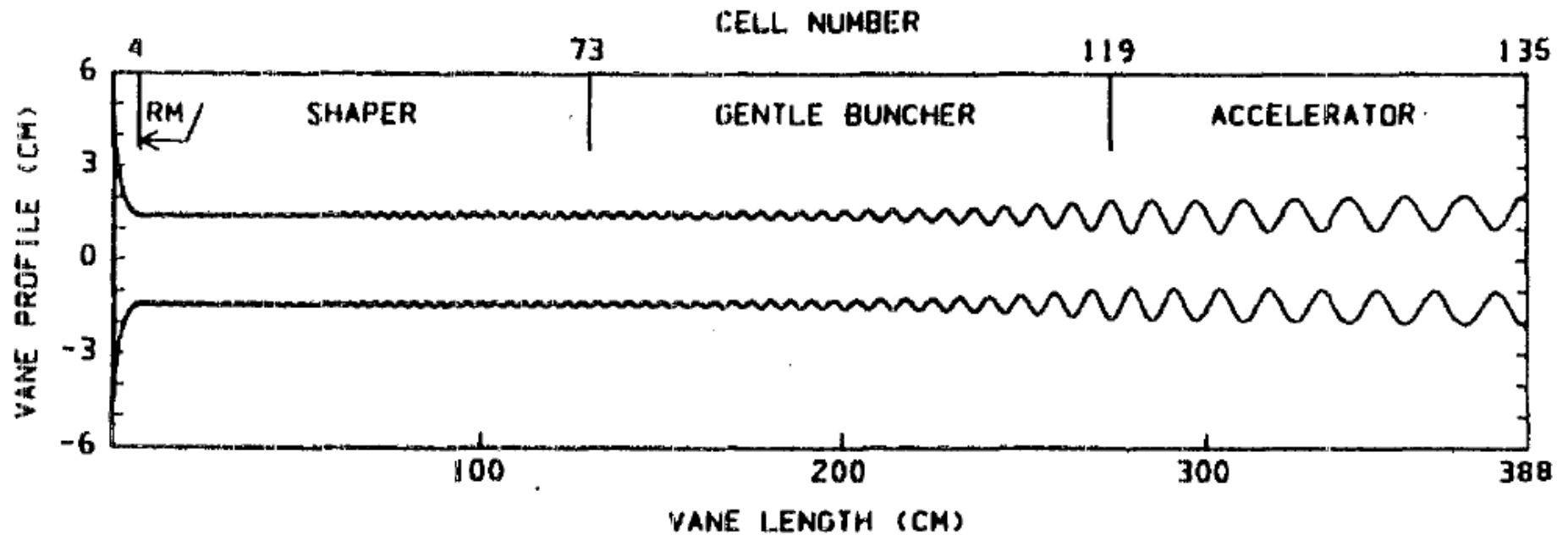
RFQ Structure

Typical RFQ design includes:
1. Radial matcher
2. Shaper (preliminary buncher with linear ramp the phase and acc. efficiency along z)
3. Gentle Buncher (quasi-stationary buncher)
4. Accelerator

Variation of RFQ Parameters Along Structure
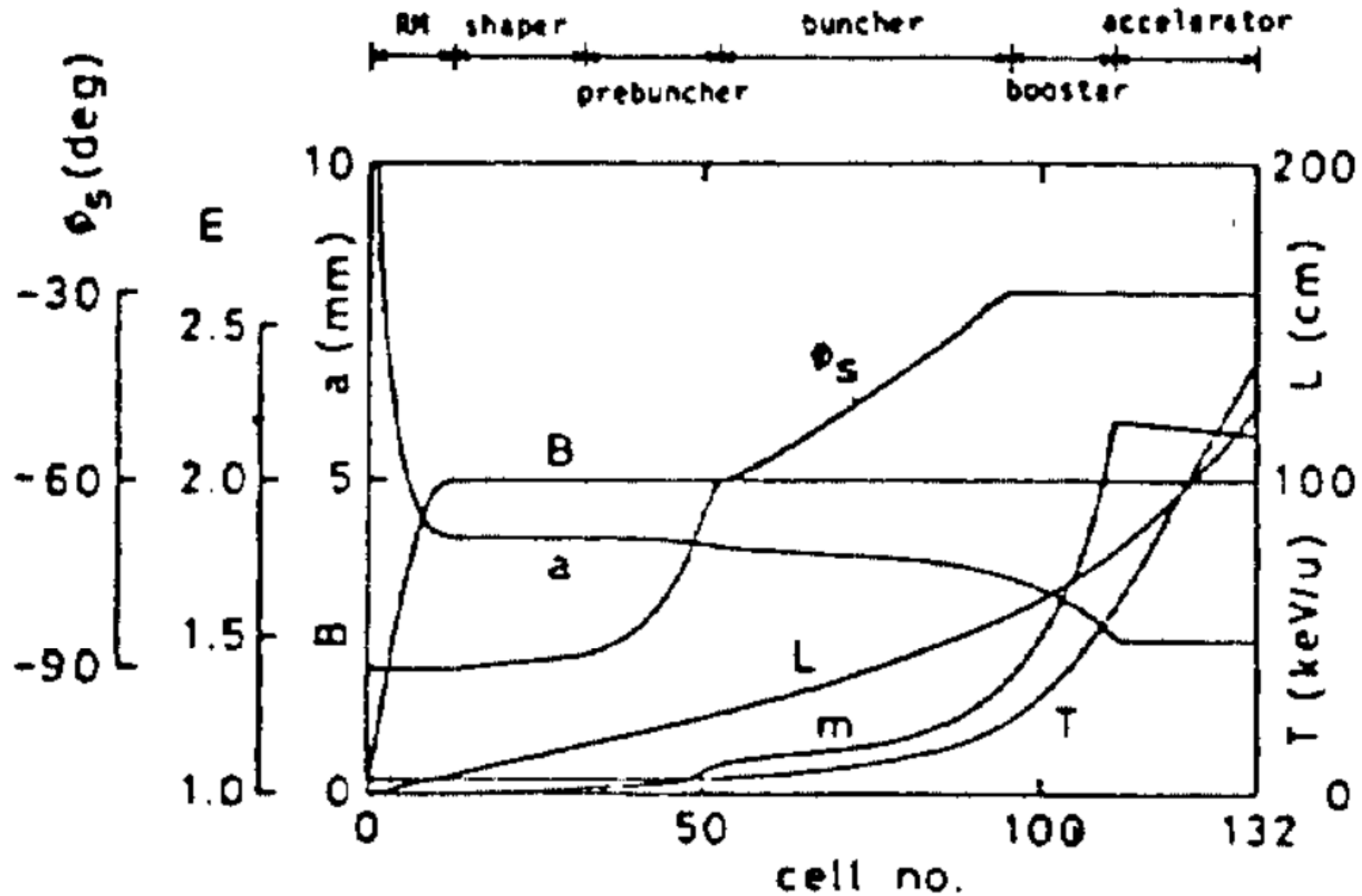

RFQ ACCELERATION CYCLE

Acceleration efficiency

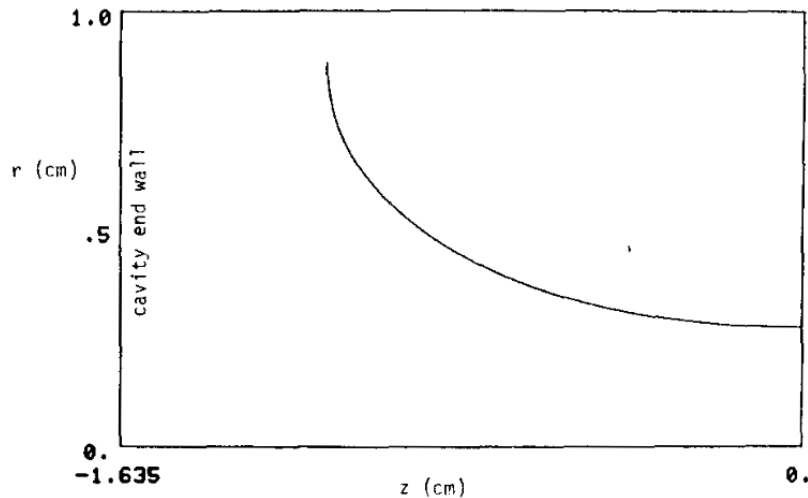$$A = \frac{4}{\pi} T$$

Rigidity of the channel

$$B = \chi \frac{qU_L}{mc^2} \frac{\lambda^2}{a^2}$$
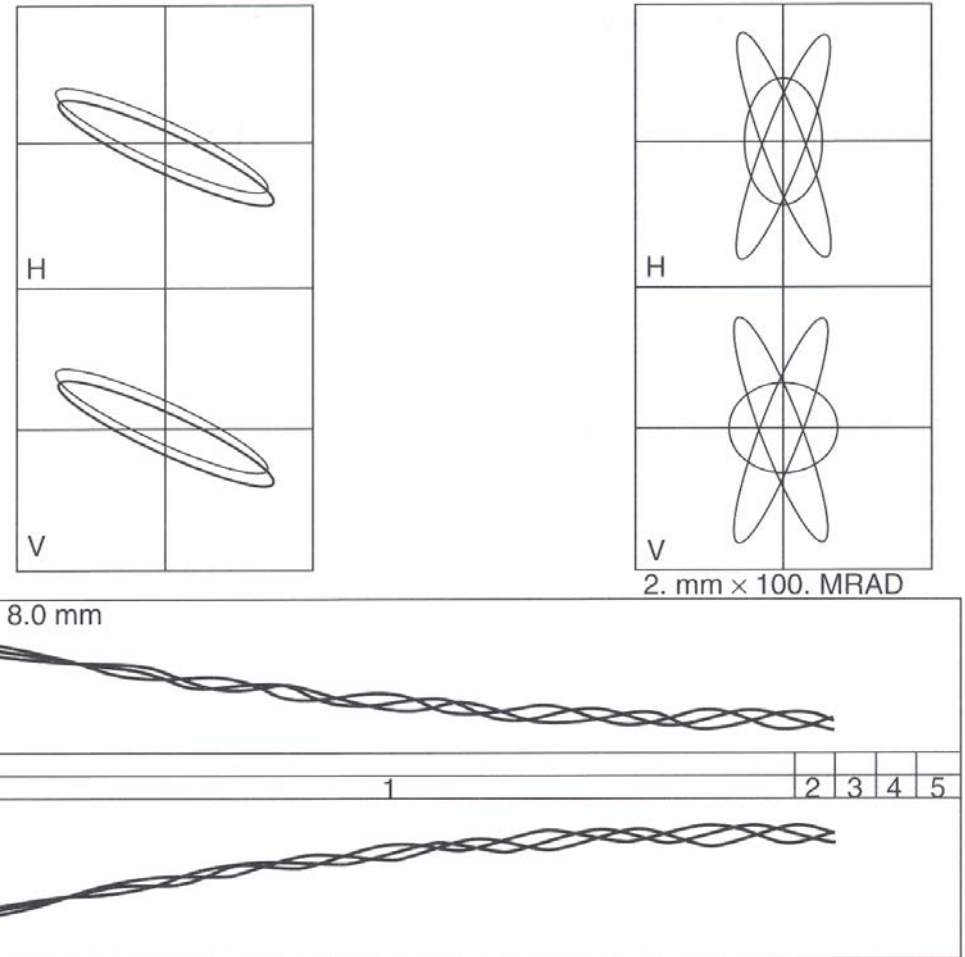
Design of RFQ Accelerator

Radial Matcher

Transforms continuous beam into time-dependent beam.
Vane radius decreases and focusing strength increases from zero to full value over a distance of few cells.

Vane profile of 3-βλ long radial matcher section (K.Crandall, 1984).

Transformation of beam envelopes in radial matcher.

Length of Buncher Section

Accelerating gradient

$$\frac{dW_s}{dz} = \frac{qU_L T \cos\varphi_s}{(\beta\lambda/2)}$$

can be re-written as
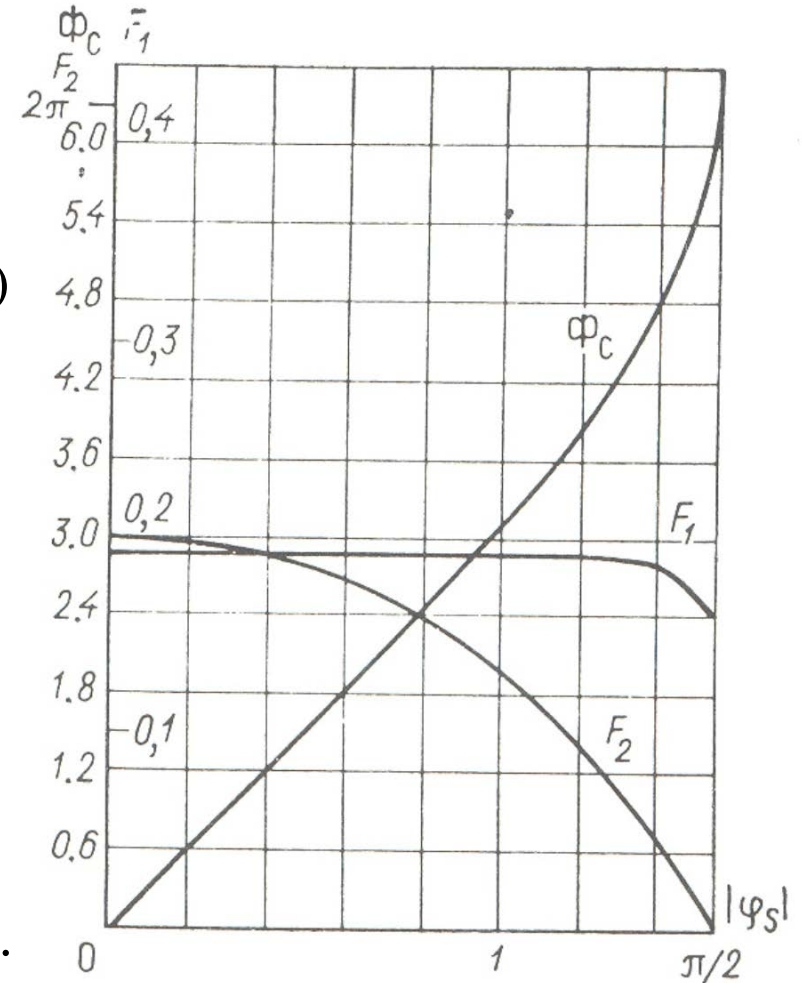
$$\frac{1}{W_s}\frac{dW_s}{dz} = \frac{2}{Z_s}(\frac{\Omega}{\omega})^2 F_2(\varphi_s)$$

where function F_2

$$F_2(\varphi_s) = \frac{\Phi_s(\varphi_s)}{tg|\varphi_s|}$$

Function F_2 can be approximated as

$$\frac{3}{F_2} = 1 + 0.3(\frac{\Phi_s}{3})^2 + 0.0964(\frac{\Phi_s}{3})^4 + 0.029(\frac{\Phi_s}{3})^6 + ...$$

Length of Buncher Section (cont.)

Length of buncher section is determined by an integral:

$$L_{buncher} = \frac{Z_s}{2}\left(\frac{\omega}{\Omega}\right)^2 \int\limits_{W_o}^{W_{fin}} \frac{dW_s}{W_s F_2(\varphi_s)}$$

Integration taking into account condition for quasi-stationary buncher

$$\boxed{\sqrt{W_s}\,\Phi_s = const}$$

gives the length of buncher:

$$\boxed{\begin{aligned}
L_{buncher} &= \frac{Z_s}{6}\left(\frac{\omega}{\Omega}\right)^2 \left\{\ln\frac{W_{fin}}{W_o} + 0.3\left(\frac{\Phi_{fin}}{3}\right)^2\left(\frac{W_{fin}}{W_o} - 1\right) + 4.8216\cdot 10^{-2}\left(\frac{\Phi_{fin}}{3}\right)^4\left[\left(\frac{W_{fin}}{W_o}\right)^2 - 1\right]+ \right. \\
&\left. + 9.643\cdot 10^{-3}\left(\frac{\Phi_{fin}}{3}\right)^6\left[\left(\frac{W_{fin}}{W_o}\right)^3 - 1\right] + 2.0548\cdot 10^{-3}\left(\frac{\Phi_{fin}}{3}\right)^8\left[\left(\frac{W_{fin}}{W_o}\right)^4 - 1\right] + ...\right\}
\end{aligned}}$$

Number of RFQ Cells in Quasi-Stationary Buncher

Increment of particle energy per per RFQ cell βλ/2

$$\frac{dW_s}{dn} = qU_L T \cos\varphi_s = 2\pi(\frac{\Omega}{\omega})^2 \frac{W_s}{tg\varphi_s}$$

Approximation of phase length of the bunch

$$\Phi_s \approx 2\pi\, tg\frac{\varphi_s}{2}$$

Condition for quasi-stationary buncher

$$\sqrt{W_s}\; tg\frac{\varphi_s}{2} = const$$

After integration, the number of RFQ cells βλ/2 in quasi-stationary buncher:

$$N = \frac{1}{\pi}(\frac{\omega}{\Omega})^2 \ln[\frac{(1-\dfrac{\Phi_{fin}}{2\pi})(1+\dfrac{\Phi_o}{2\pi})}{(1+\dfrac{\Phi_{fin}}{2\pi})(1-\dfrac{\Phi_o}{2\pi})}]$$

Length of RFQ Accelerator Section

In accelerator section, synchronous phase $\varphi_s = const$, and acceleration efficiency T is approximately constant:

$$T \approx \frac{\pi}{4}\left(\frac{m^2 - 1}{m^2 + 1}\right)$$

Energy gain per cell is constant:

$$\Delta W_s = qU_L T \cos\varphi_s = const$$

Accelerating gradient can be written as

$$\frac{dW_s}{dz} = \frac{\Delta W_s}{(\beta\lambda/2)} = \frac{\sqrt{2mc^2}}{\lambda}\frac{\Delta W_s}{\sqrt{W_s}}$$

Integration gives the length of RFQ accelerator section:

$$L_{acc} = \frac{\lambda}{\sqrt{2mc^2}\,\Delta W_s} \int_{W_{o\_acc}}^{W_{fin\_acc}} \sqrt{W_s}\, dW_s$$

$$\boxed{L_{acc} = \frac{\sqrt{2}}{3}\frac{\lambda mc^2}{\Delta W_s}\left[\left(\frac{W_{fin\_acc}}{mc^2}\right)^{3/2} - \left(\frac{W_{o\_acc}}{mc^2}\right)^{3/2}\right]}$$

Los Alamos
NATIONAL LABORATORY

Transition Cell

Transition cell makes a smooth transition from full modulation at the last accelerating cell to no modulation and pure quadrupole symmetry at the end of the transition cell (K.Crandall, 1994).
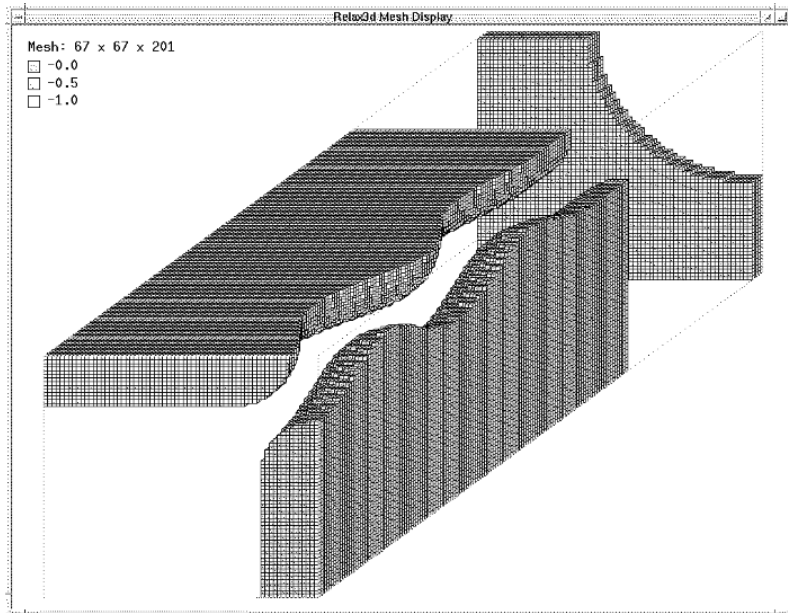
Three regular cells, a transition cell and a short unmodulated
end section of ISAC RFQ at TRIUMF (S. Koscielniak et al, PAC97).
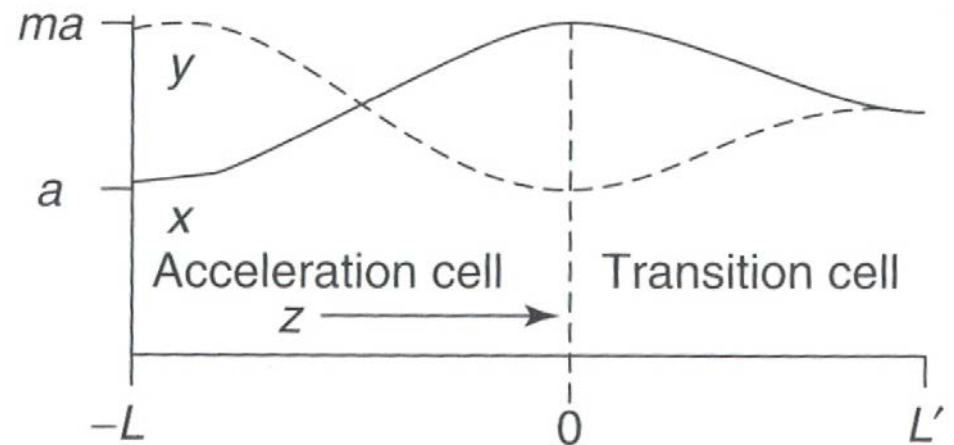
Vane-tip profile in final accelerating cell followed by a transition cell.

Radial RFQ Dynamics

Transverse particle oscillation in an RF field in the smooth approximation

$$\frac{d^2 x}{dt^2} + x[\Omega_{rs}^2 - \frac{\Omega^2}{2}\,ctg\,\varphi_s \Phi \sin(\Omega t + \psi_o)] = 0$$

Transverse oscillation frequency of a synchronous particle in the presence of an RF field. Stability of transverse oscillations requires $\Omega_{rs} > 0$

$$\Omega_{rs}^2 = \Omega_r^2 - \frac{\Omega^2}{2}$$

$$\Omega_r > \frac{\Omega}{\sqrt{2}}$$

$$\frac{qU_L}{W_s} > \frac{32\pi^3 T}{\chi^2}(\frac{a}{\beta\lambda})^4$$

Parametric resonance occurs when $a = n^2$

$$\Omega_{rs} = \frac{n}{2}\Omega, \quad n = 1, 2, 3$$

In an RFQ linac, the transverse oscillation frequency is typically larger than the longitudinal oscillation frequency, and the first parametric resonance instability region is avoided. The potentially dangerous region in this case is the second parametric resonance bandwidth where $n = 2$. Instabilities of higher-order resonance regions are typically unimportant.

Los Alamos
NATIONAL LABORATORY

Transverse Acceptance

Phase advance of synchronous particle $\mu_s = \Omega_{rs}\lambda/c$

$\mu_s = \Omega_{rs}S/\beta c$ per focusing period $S = \beta\lambda$

$$\mu_s^2 = \frac{B^2}{8\pi^2} - 2\pi^2 \left(\frac{\Omega}{\omega}\right)^2$$

Rigidity of channel

$$B = \chi \frac{qU_L}{mc^2} \frac{\lambda^2}{a^2}$$

Transverse un-normalized acceptance

$$A = \frac{a^2 \mu_s}{S\,(1+\upsilon_{max})^2} = \frac{a^2 \mu_s}{\beta\lambda\,(1+\upsilon_{max})^2}$$

From averaging method

$$\upsilon_{max} = \frac{|\xi_{max}|}{x}$$

$$\xi = -\frac{f_1}{m\omega^2}$$

$$f_1 = \chi \frac{qU_L\,x}{a^2}$$

$$\upsilon_{max} = \frac{B}{4\pi^2}$$

Transverse normalized acceptance

$$\varepsilon_{ch} = \gamma \frac{a^2}{\lambda} \frac{\mu_s}{\left(1+\dfrac{B}{4\pi^2}\right)^2}$$

Beam Current Limits in RFQ

RFQ focusing period

$$S = \beta\lambda$$

RFQ amplitude of equivalent traveling wave

$$E = 2\frac{U_L T}{\beta\lambda}$$

Transverse current limit

$$I_{\max,\, t} = \frac{I_c}{3\pi}\beta\left(\frac{a}{\lambda}\right)^2 \frac{\mu_s^2\,|\varphi_s|}{(1-M_z)}\,[1-\left(\frac{\varepsilon}{\varepsilon_{ch}}\right)^2]$$

Longitudinal current limit

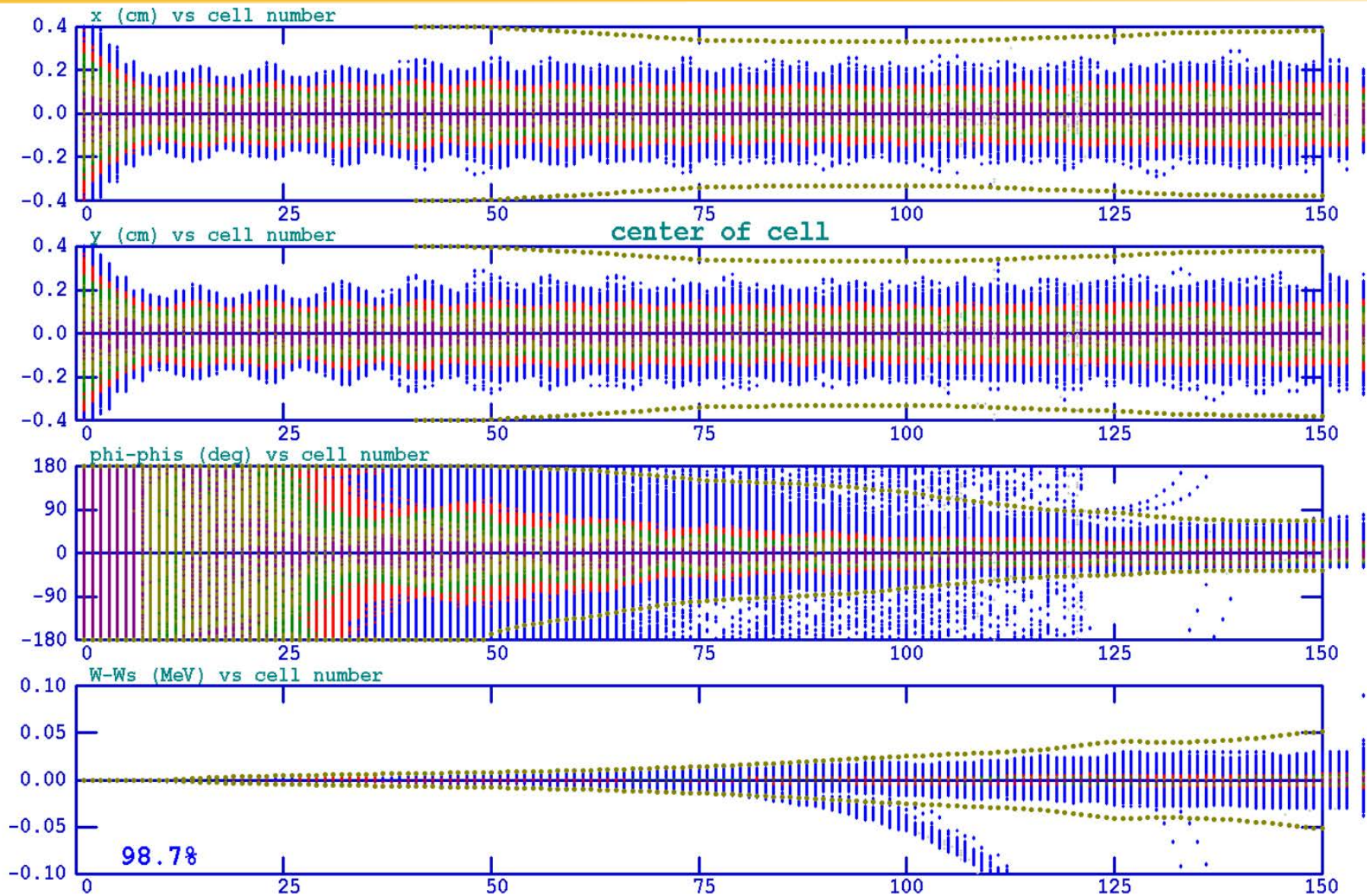$$I_{max,l} = I_c \left(\frac{qU_L T}{mc^2}\right)\frac{\varphi_s^2 \sin\varphi_s}{\pi}\left(\frac{a}{\lambda}\right)\left(1-\frac{\varepsilon_z^2}{\varepsilon_{acc}^2}\right)$$

Approximate longitudinal normalized acceptance

$$\varepsilon_{acc} = \frac{1}{2\pi}\beta^2\left(\frac{\Omega}{\omega}\right)\varphi_s^2\,\lambda$$

Los Alamos
NATIONAL LABORATORY

Macroparticle Dynamics in RFQ

Beam dynamics in 35keV/750keV/35mA proton RFQ (Courtesy of Larry Rybarcyk).
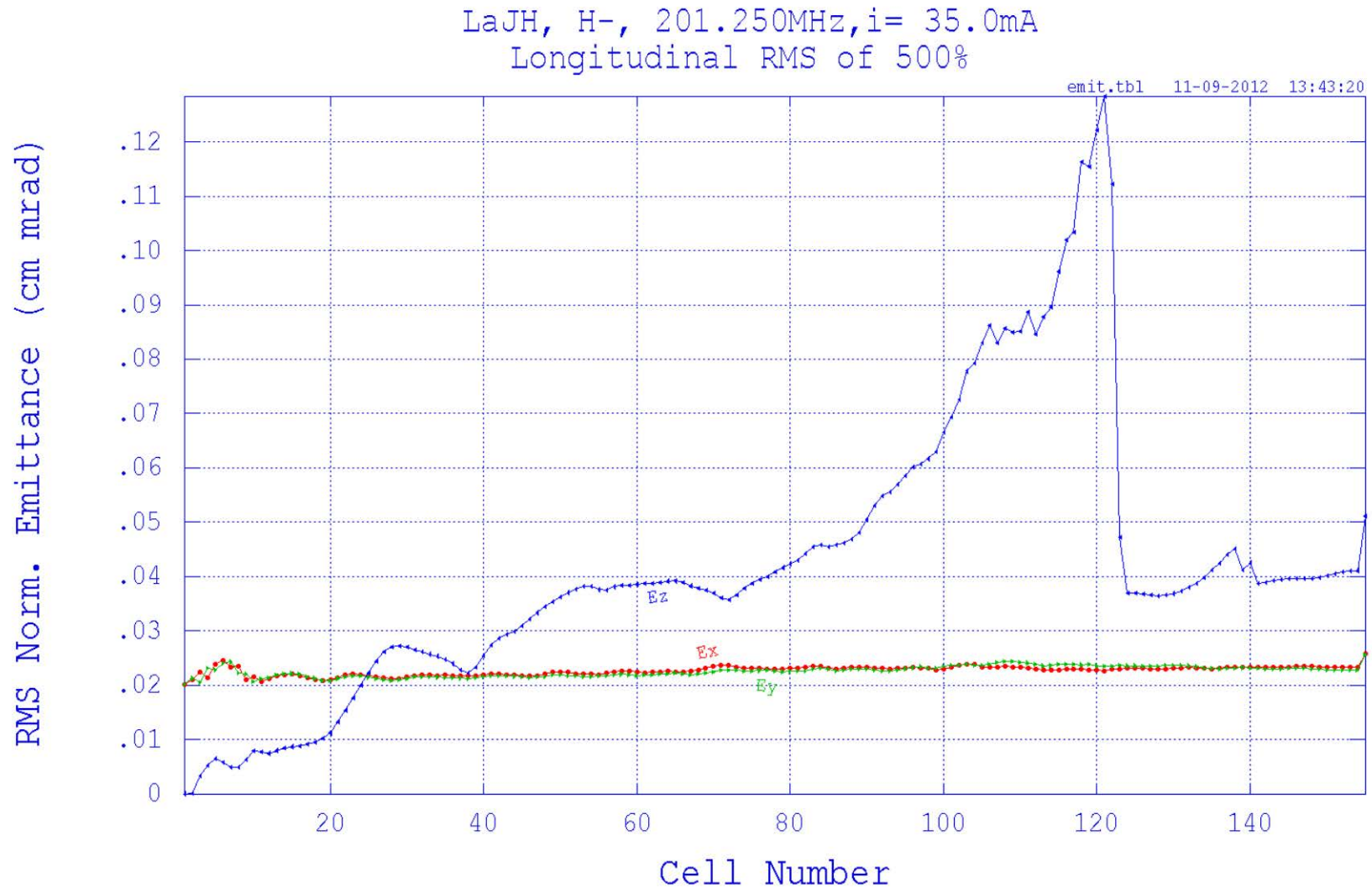
Los Alamos
NATIONAL LABORATORY

Macroparticle Dynamics in RFQ (cont.)
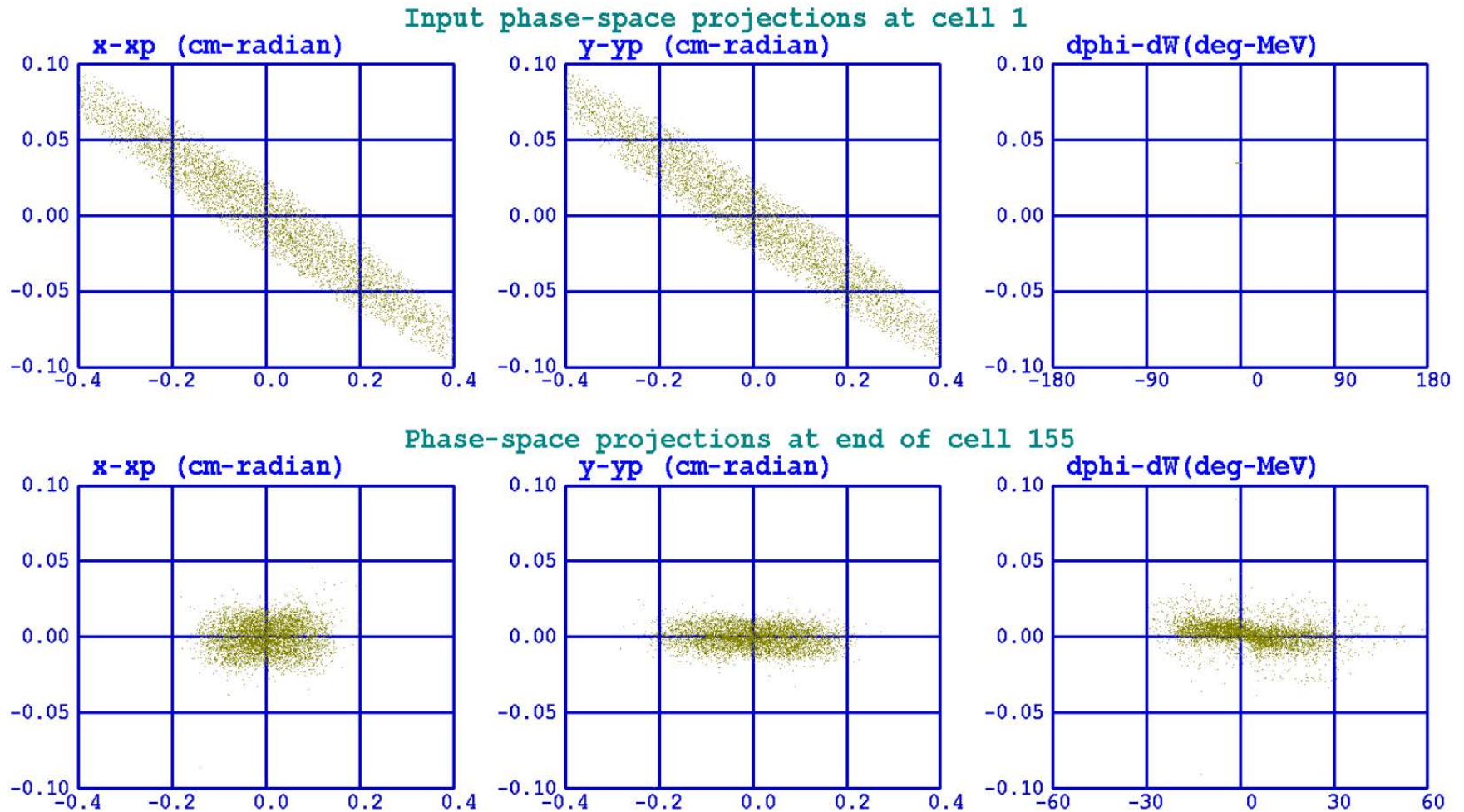
Input and output beam distributions in 35keV/750keV/35mA proton RFQ.

Macroparticle Dynamics in RFQ (cont.)

Transverse and longitudinal emittance growth in 35keV/750keV/35mA proton RFQ.

Longitudinal Parametric Resonance in RFQ

Injection of low-velocity particles into an RFQ results in dependence of the longitudinal oscillation frequency on transverse particle position.

Equation of small-amplitude longitudinal oscillations for off-axis particles

$$\frac{d^2\zeta}{dt^2} + \Omega^2 I_o(k_z r)\zeta = \frac{\Omega^2}{k_z|tg\varphi_s|}[I_o(k_z r) - 1]$$

Averaged transverse oscillations can be approximated by

$$r = R\cos\Omega_{rs}t$$

Periodic function can be expanded in Fourier series

$$I_o(k_z R\cos\Omega_{rs}t) = I_o^2(\frac{k_z R}{2}) + 2\sum_{m=1}^{\infty} I_m^2(\frac{k_z R}{2})\cdot\cos 2m\Omega_{rs}t$$

Because the amplitudes of the terms of the Bessel function drop off quickly, only the first two terms are important, resulting in the following equation of motion

$$\frac{d^2\zeta}{dt^2} + \Omega^2\zeta[I_o^2(\frac{k_z R}{2}) + 2I_1^2(\frac{k_z R}{2})\cdot\cos 2\Omega_{rs}t] = \frac{\Omega^2}{k_z tg\varphi_s}[I_o^2(\frac{k_z R}{2}) - 1 + 2I_1^2(\frac{k_z R}{2})\cos 2\Omega_{rs}t]$$

Los Alamos
NATIONAL LABORATORY

Longitudinal Parametric Resonance in RFQ (cont.)

Analysis of longitudinal parametric instabilities includes

(i) consideration of a Mathieu-type equation parametric resonance instability neglecting the right-side part equation

(ii) external resonances, taking into account the right-hand external driving force of equation

Longitudinal parametric resonances occur when the following condition is fulfilled:

$$\frac{\Omega_{rs}}{\Omega} = \frac{I_o(\frac{k_z R}{2})}{n} \qquad n = 1, 2, 3,...$$

with the region of parametric instability defined as:

$$\frac{I_o^2(\frac{k_z R}{2})}{a_n} < (\frac{\Omega_{rs}}{\Omega})^2 < \frac{I_o^2(\frac{k_z R}{2})}{b_n}$$

Los Alamos
NATIONAL LABORATORY

Longitudinal Parametric Resonance in RFQ (cont.)

where a_n, b_n determine Mathieu stability regions, and the parameter

$$q = (\frac{\Omega}{\Omega_{rs}})^2 I_1^2 (\frac{k_z R}{2}) .$$

The first significant parametric resonance area is when $n = 1$. This leads to the following resonance bandwidth

$$I_o^2 (\frac{k_z R}{2}) - I_1^2 (\frac{k_z R}{2}) < (\frac{\Omega_{rs}}{\Omega})^2 < I_o^2 (\frac{k_z R}{2}) + I_1^2 (\frac{k_z R}{2}) .$$

Longitudinal Parametric Resonance in RFQ (cont.)

Consider conditions for excitation of external resonance. When parametric resonance conditions are not fulfilled, one can neglect frequency modulation, because $I_1^2(k_z R/2) << I_o^2(k_z R/2)$. Equation of longitudinal oscillations is

$$\frac{d^2\zeta}{dt^2} + \zeta\,\Omega^2 I_o^2(\frac{k_z R}{2}) = \frac{\Omega^2}{k_z\,tg\,\varphi_s}[I_o^2(\frac{k_z R}{2}) - 1 + 2I_1^2(\frac{k_z R}{2})\cos 2\Omega_{rs}t]$$

An external resonance occurs when the transverse oscillation frequency is $\Omega_{rs} = \frac{\Omega}{2}\,I_o(k_z R/2)$. Both external and parametric resonances can be avoided simultaneously when

$$\boxed{\frac{\Omega_{rs}}{\Omega} > I_o(\frac{k_z a}{2})}$$

Los Alamos
NATIONAL LABORATORY

Parametric Resonance in RFQ

avoiding parametric resonances

a)

$U_L = 72.6\ kV$

χ

m

$a(cm)$ T

b)

$\dfrac{\Omega_{rs}}{\Omega}$

c)

$\varepsilon\ (\pi\ cm\ mrad)$

ε_z

$\varepsilon_{x,y}$

d)

η

including parametric resonances

$U_L = 91.6\ kV$

χ

m

$a(cm)$ T

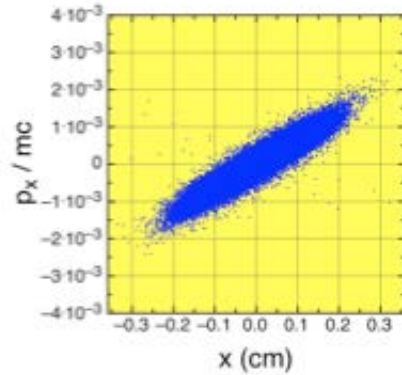$\dfrac{\Omega_{rs}}{\Omega}$

ε_z

$\varepsilon_{x,y}$

η
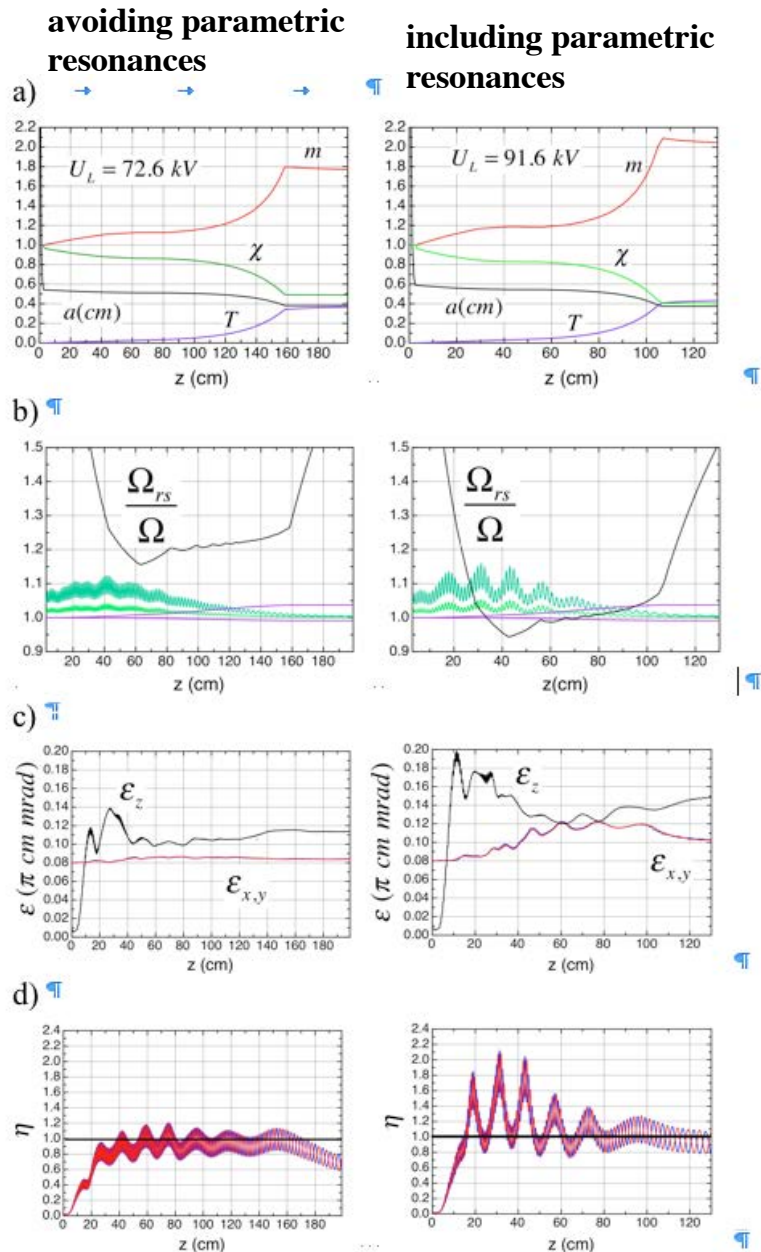
Fig. 4. Beam dynamics in RFQ with beam current $I = 35$ mA: (left) avoiding parametric resonances, (right) including parametric resonances: (a) RFQ parameters, (b) parametric resonance bandwidth: (green) Eq. (18), (red) Eq. (9), (c) beam emittances, (d) equipartitioning parameter, Eq. (5).

avoiding parametric resonances

including parametric resonances

Y.B. et al (IPAC2013)
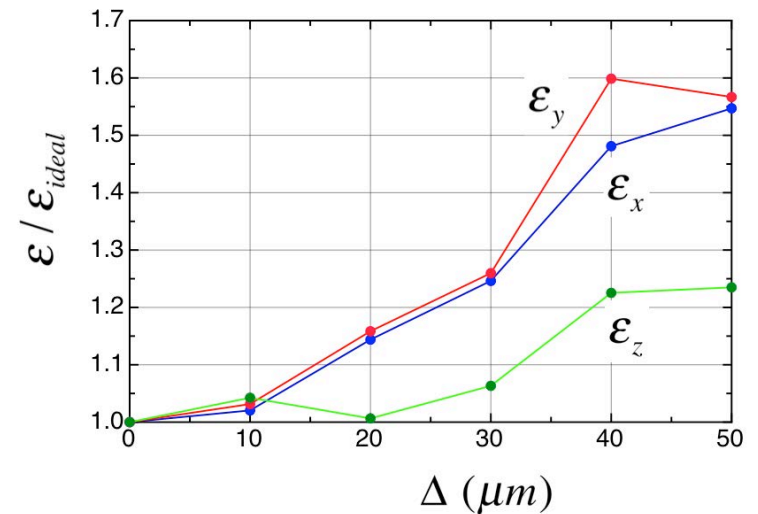
41
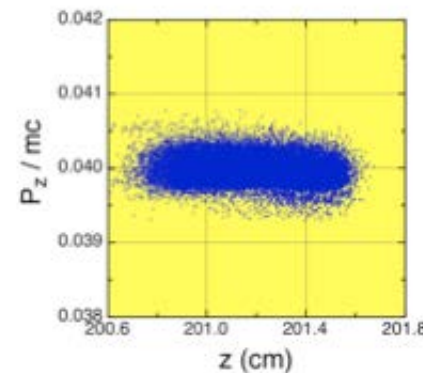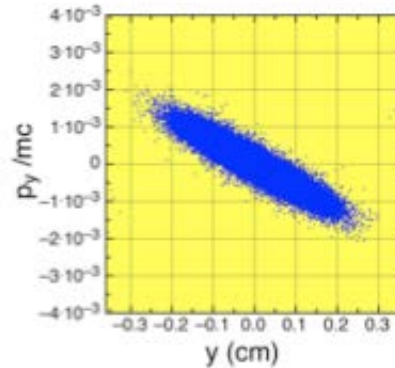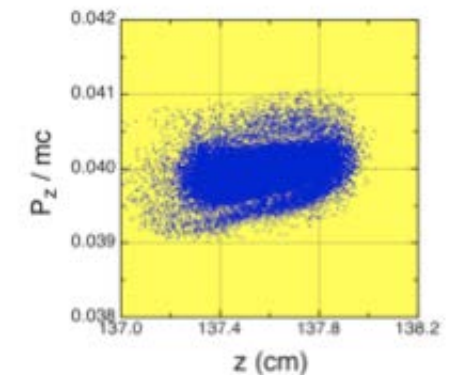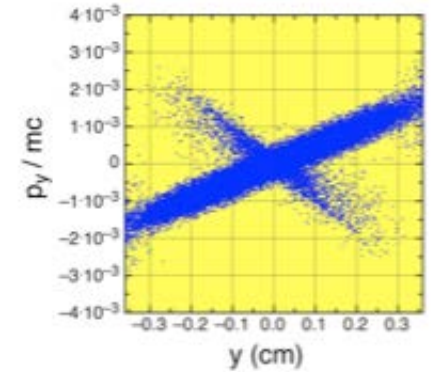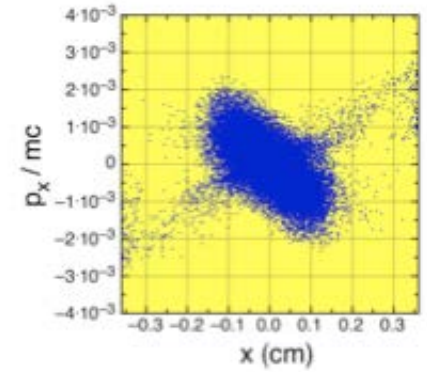
Effect of Random Errors

Increase of the amplitude of longitudinal oscillations at each cell due to random errors

$$\frac{<\delta p_z>^2}{P_z^2} = \frac{\pi^2}{2}(\frac{\Omega}{\omega})^4 ctg^2\varphi_s(<\frac{\delta U_L}{U_L}>^2 + <\frac{\delta T}{T}>^2) + \frac{\pi^2}{2}(\frac{\Omega}{\omega})^2[1+\pi^2(\frac{\Omega}{\omega})^2]<\frac{\delta L}{L}>^2$$

Increase of the transverse amplitude of particle oscillations at each cell

$$<\frac{\delta R}{R}>^2 = 2(<\frac{\delta r_o}{R}>^2 + <\frac{\delta U_L}{U_L}>^2 + 4<\frac{\delta R_o}{R_o}>^2)$$
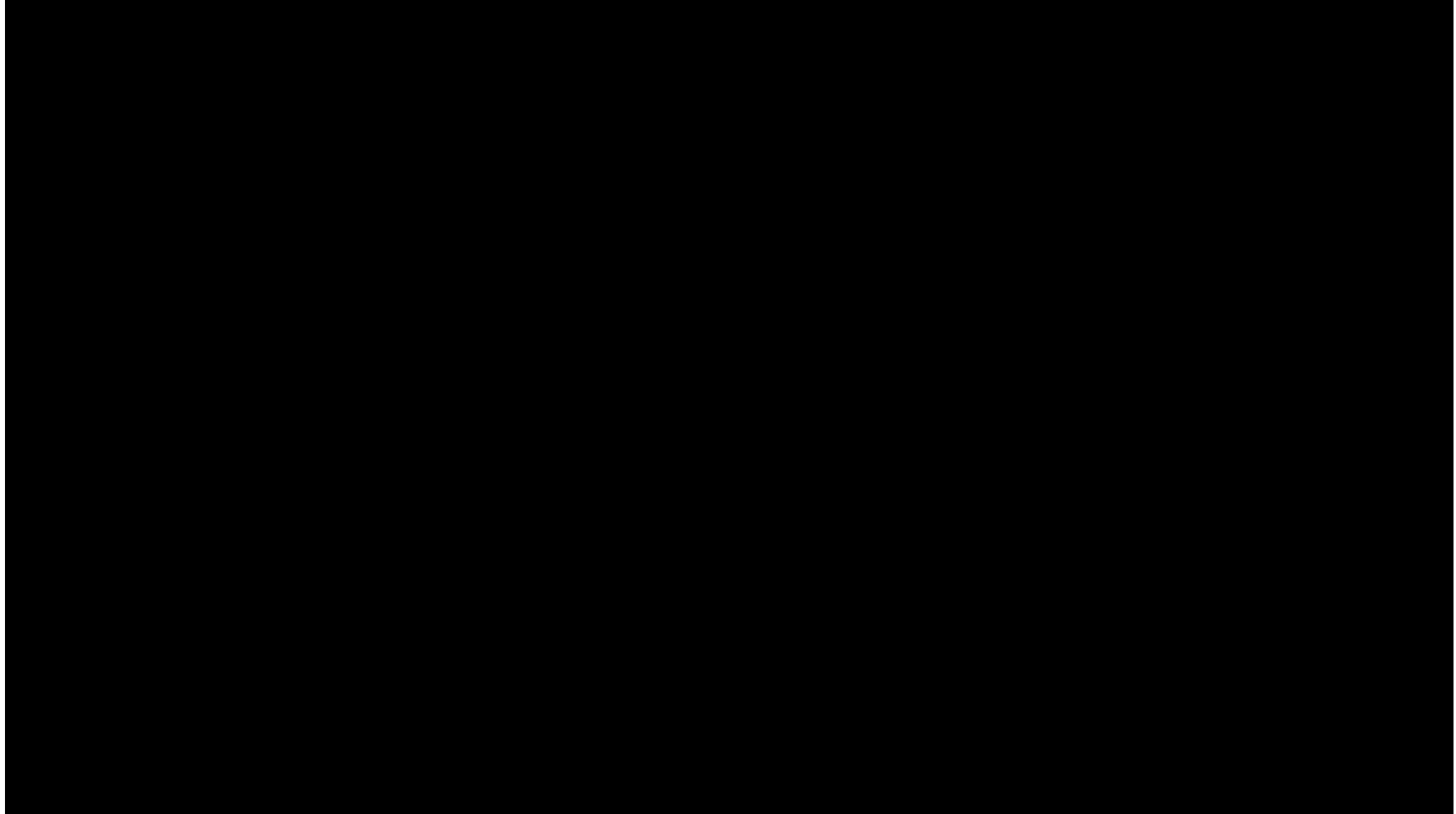
Typical limitations in RFQ vane tips manufacturing errors is Δ = 20 – 30 microns.

Effect of manufacturing errors on beam emittance.

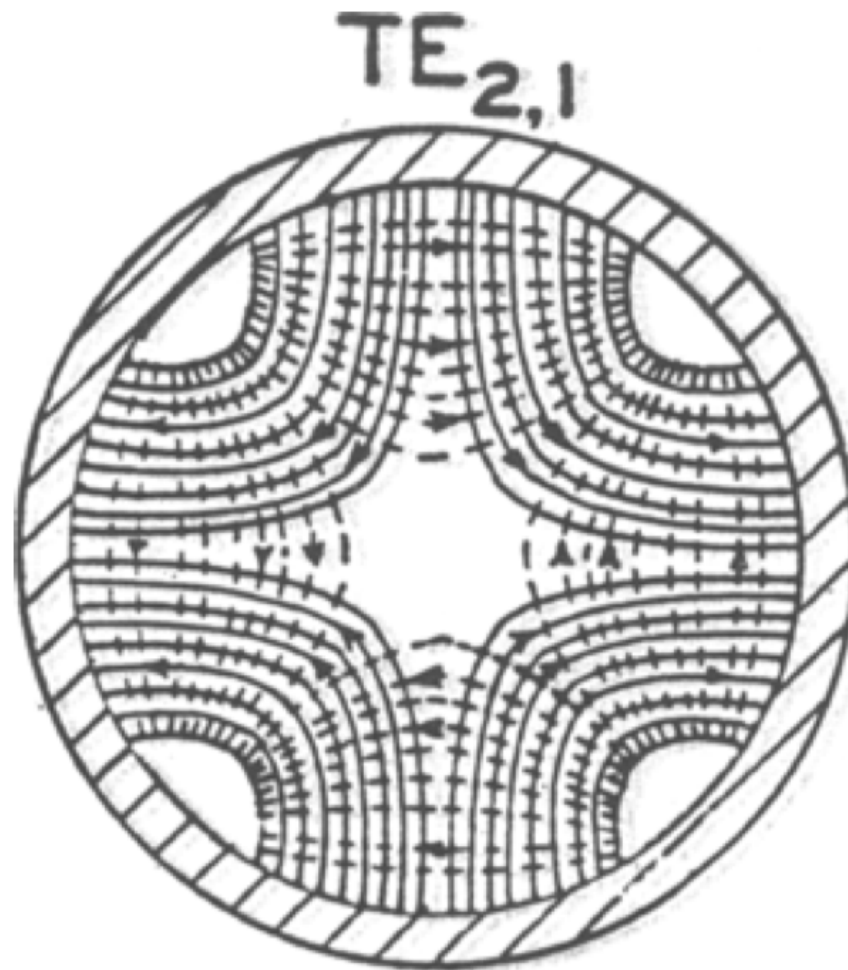Los Alamos
NATIONAL LABORATORY

Example of RFQ Beam Dynamics

Dynamics of 35 mA proton beam in 201.25 MHz 4-rod RFQ (courtesy of Sergey Kurennoy).
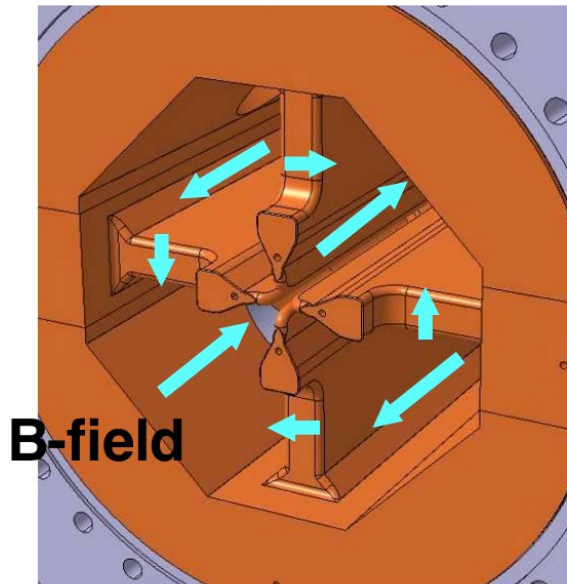
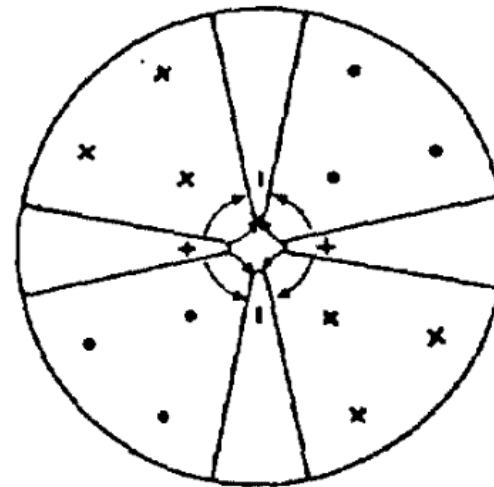# Design of RFQ Cavities

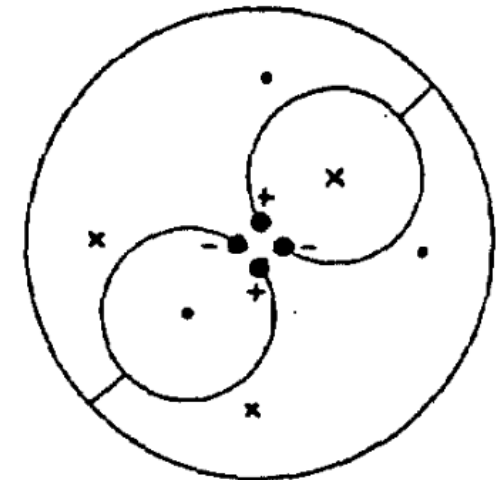Circular Waveguide Excited by TE21 Mode

Resonant RFQ Cavities

Transverse electric field is localized near vane tips.
Magnetic field is longitudinal localized in four outer quadrants.

B-field

End-cell of a four-vane RFQ.
The arrows show the direction
of the magnetic field
(M.Vretenar).

Four Vane Resonator
(TE$_{210}$ - like)

Double-H-Resonator
(2 · TE$_{110}$ - like)

Cross sections of RFQ cavities.

A major drawback of the four-vane structure is
its sensitivity to mechanical errors.

4 Vane - RFQ
H_{210} - mode
$f \gtrsim 100$ MHz

IH - RFQ
H_{110} - mode
$f \lesssim 100$ MHz

$$\emptyset_{IH}\ (f) \sim 0.45\ \text{x}\ \emptyset_{4\ Vane}\ (f)$$
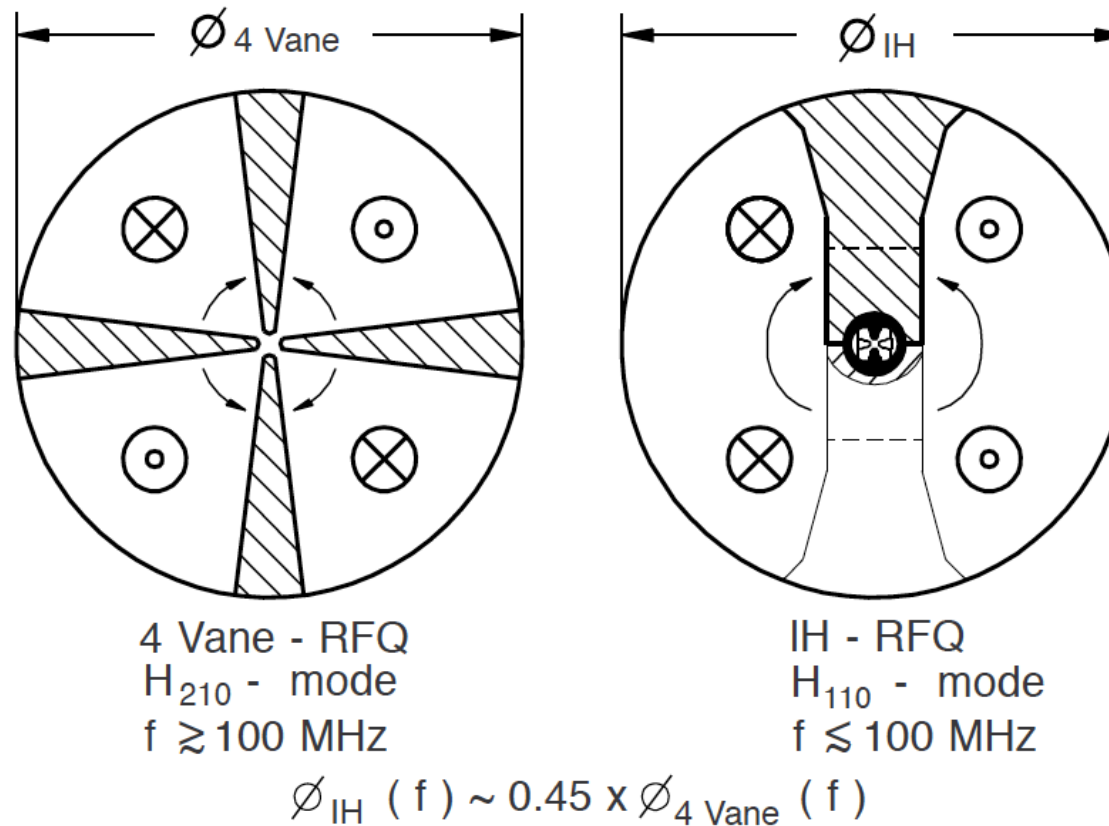
Fig. 3. Simplified cross-sections of the 4 Vane-RFQ and of the IH-RFQ with corresponding field orientations.

H-type accelerating structures (U.Ratzinger, Linac96).

1972 First Demo RFQ (Protvino, Russia)

Demo RFQ (IHEP, Protvino, Moscow Region, Russia)
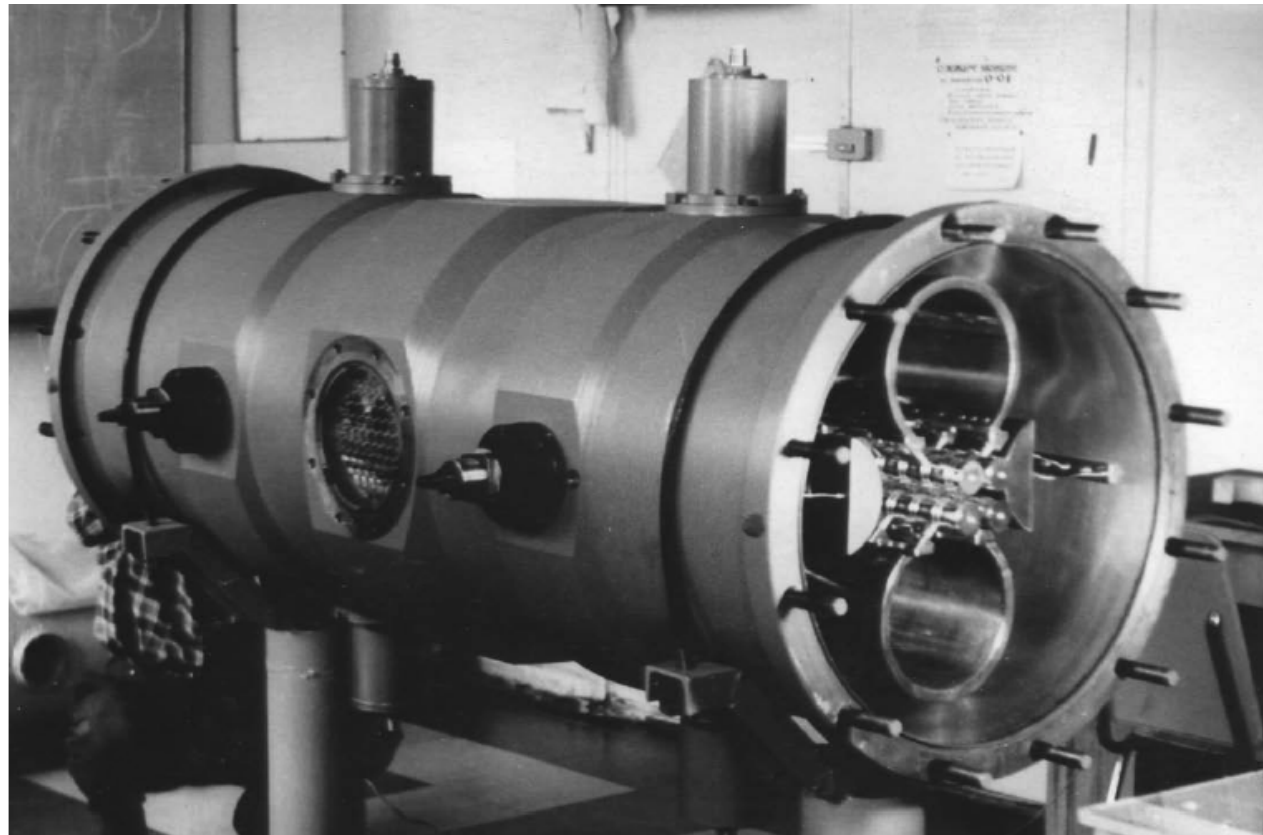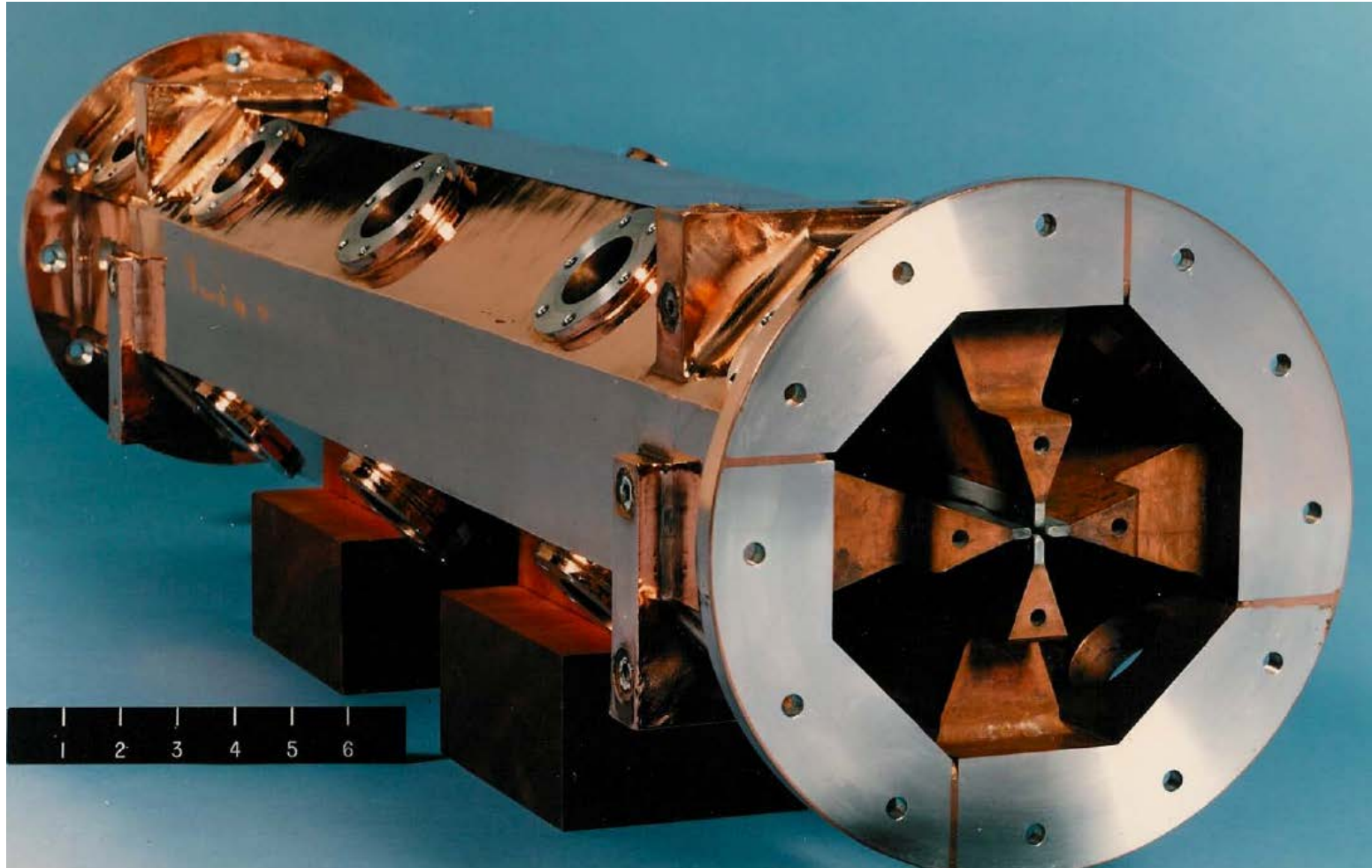
    1972

    100 – 620 keV, 200 mA, protons

    148.5 MHz, 0.0025 % duty

    Cu-plated carbon steel cavity, brazed OFE Cu vanes

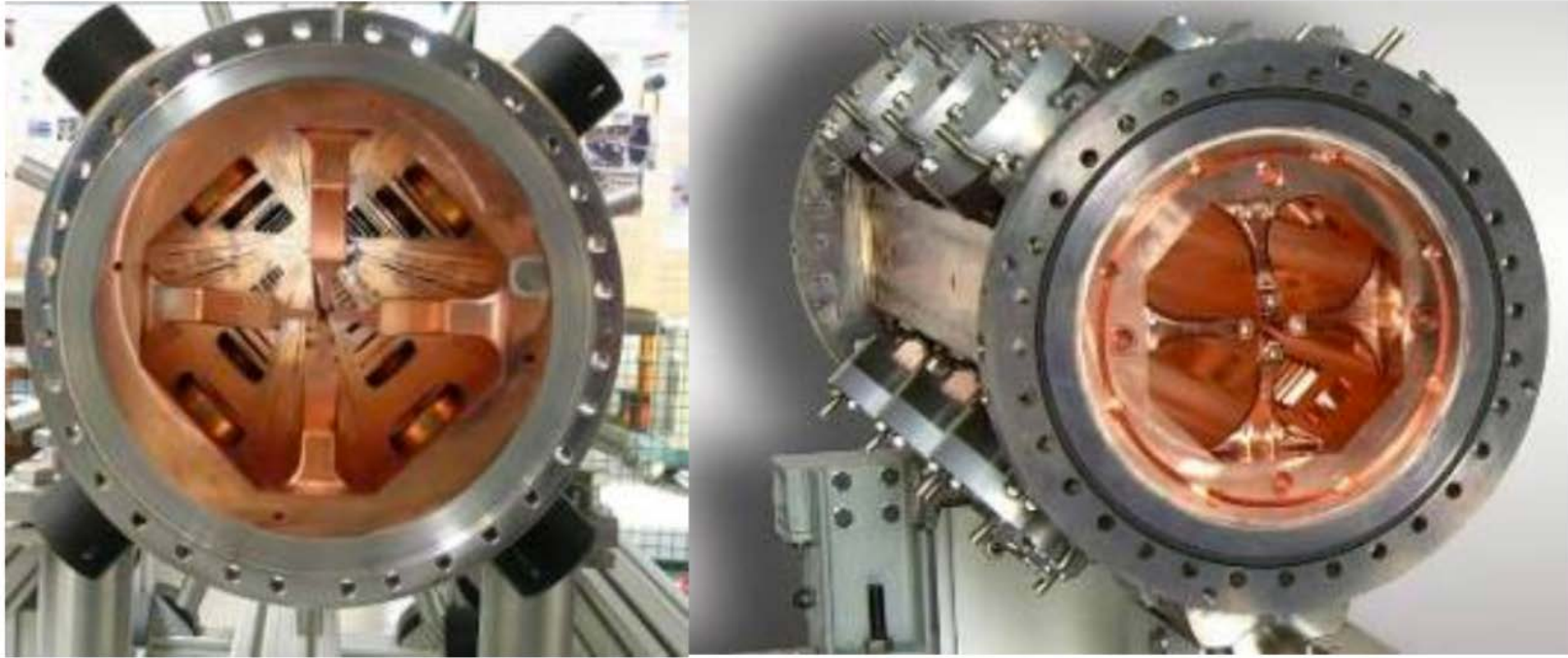   First operational RFQ, H-mode cavity

"BEAR" RFQ (LANL, 1989)

BEAR" 30-keV to 1-MeV, 1-m long, 425-MHz, 30 mA H- RFQ operated in space for SDI missile defense program (1989). This RFQ is now in the Smithsonian.
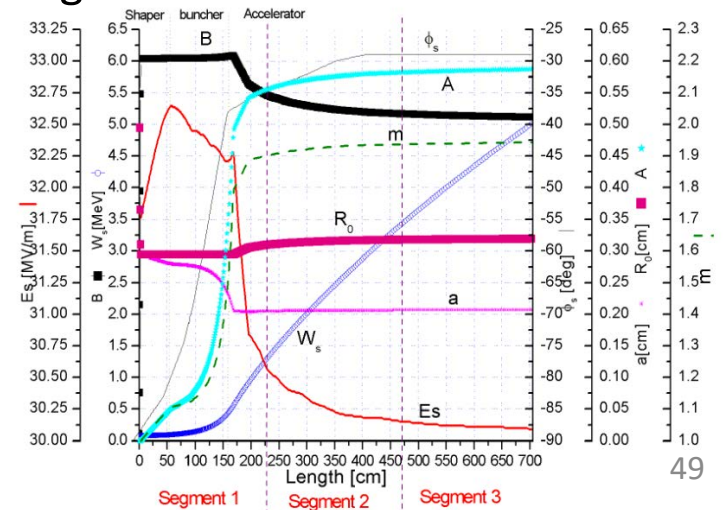
Los Alamos
NATIONAL LABORATORY

CW European RFQ

The first two modules of TRASCO and the first module of IPHI RFQ.

Table 1 RFQ specifications

TRASCO RFQ Design

Particle	p	
Input Energy	80	KeV
Output Energy	5	MeV
Frequency	352.2	MHz
Current	30	mA
Max Surface Field	33	MV/m
RF Power consumption	<800	kW
Duty factor	100	%

Los Alamos
NATIONAL LABORATORY
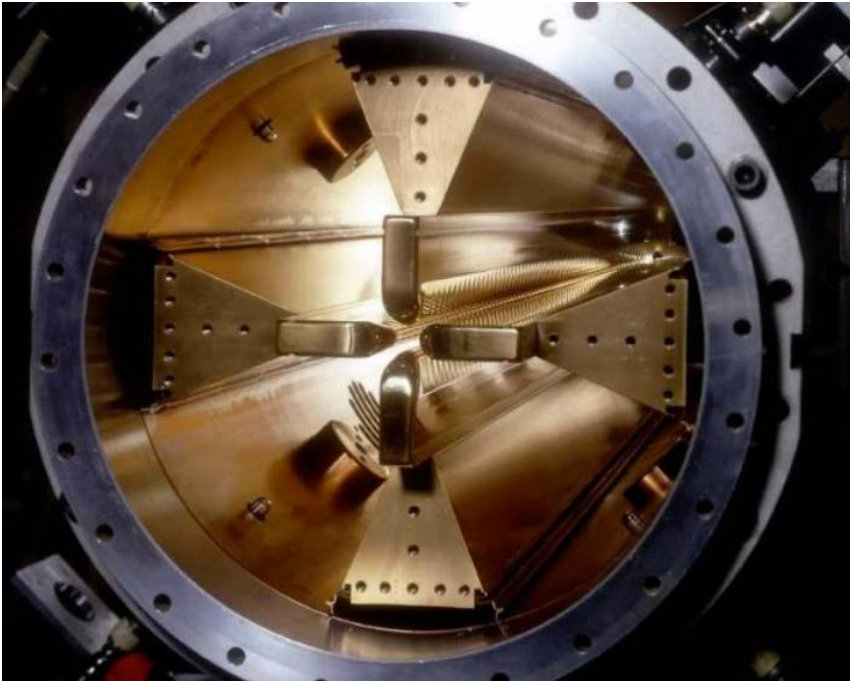
CERN RFQs

RFQ for CERN LINAC4, 352 MHz

CERN RFQ1, 202 MHz

Figure 2: 3rd RFQ module.

Los Alamos
NATIONAL LABORATORY
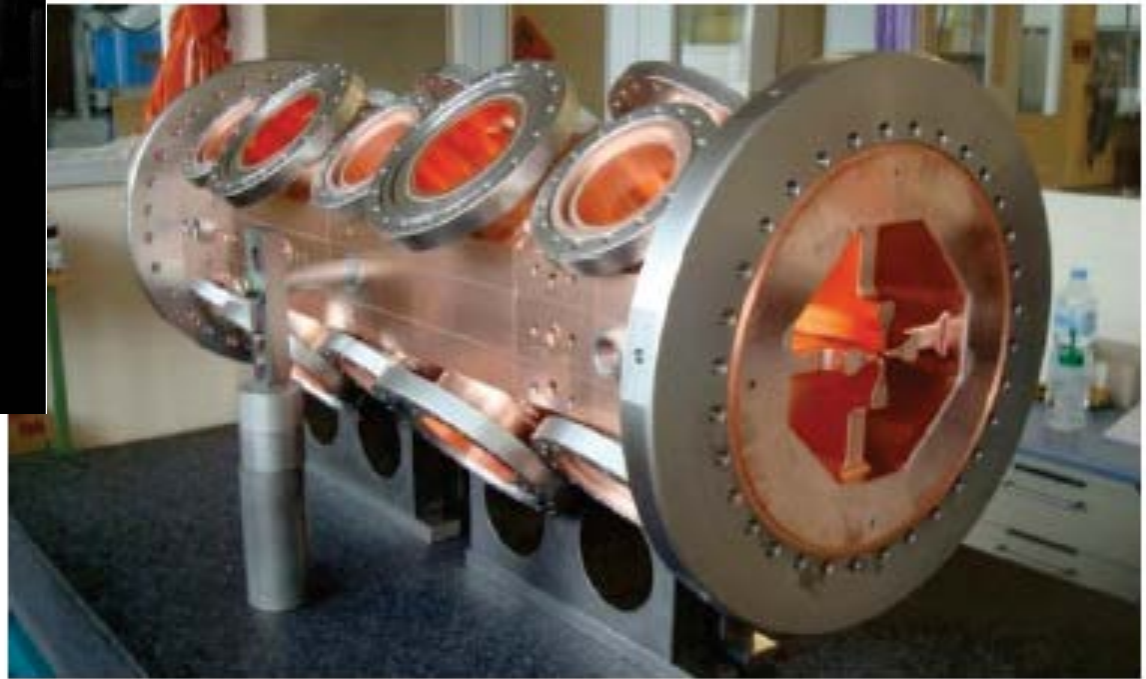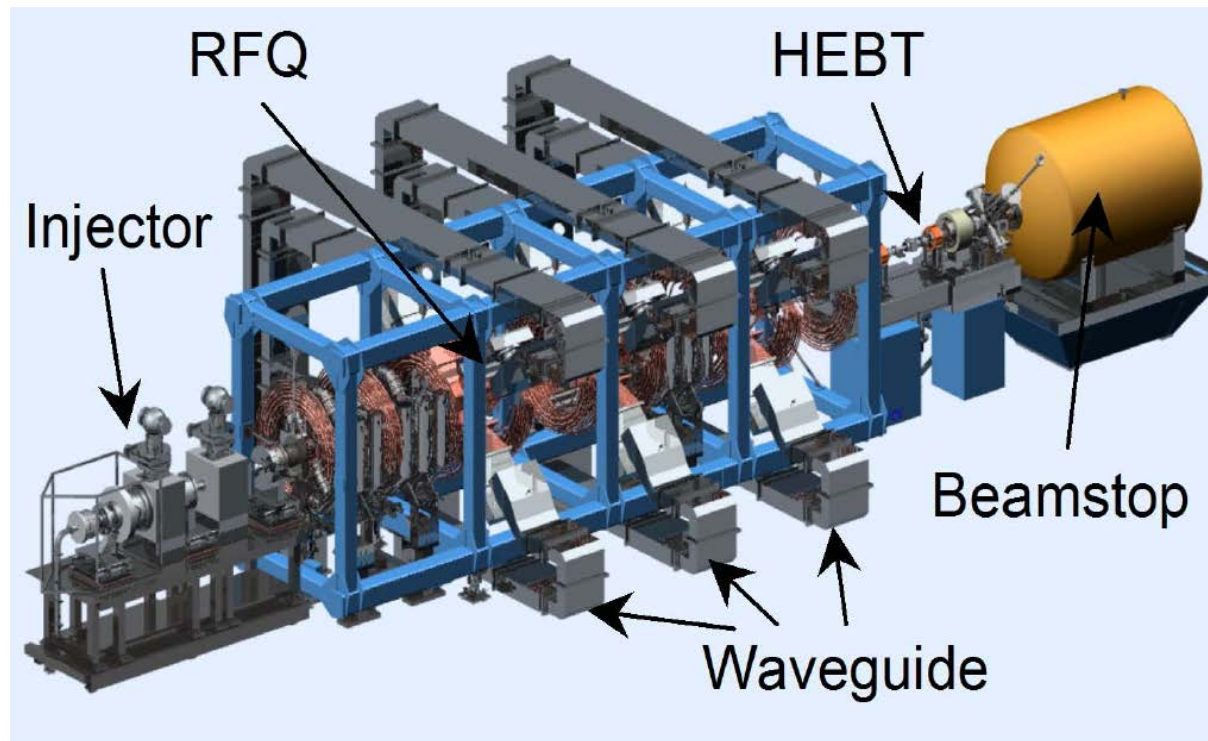
LEDA RFQ (LANL, 1999)

Most powerful RFQ was 350-MHz 8-m long CW RFQ that accelerated a 100-mA proton beam at Los Alamos (LEDA) from 75-keV to 6.7-MeV

Los Alamos
NATIONAL LABORATORY

Suppression of Unwanted RFQ Modes

Mismatch of the resonant frequencies of the four quadrants results in unequal excitation, exciting dipole modes, which interfere with the acceleration of the beam.
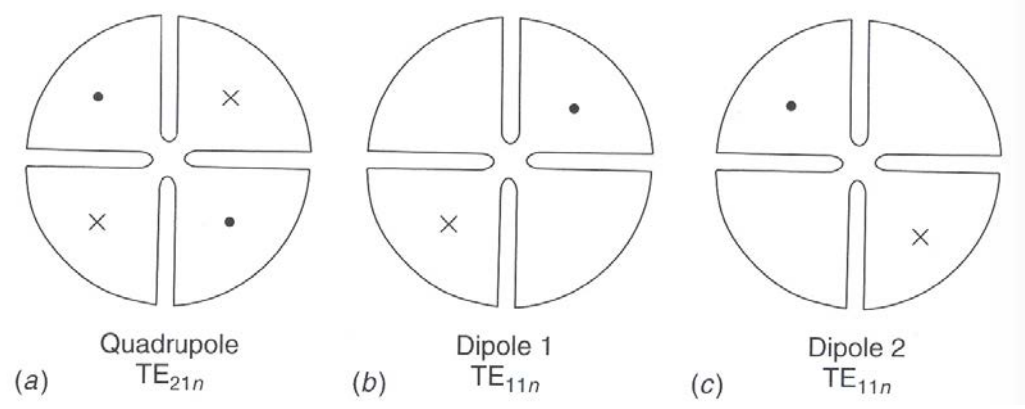
RFQ structures are susceptible to errors in the longitudinal voltage distribution:

$$\frac{\partial^2}{\partial z^2}\left(\frac{\delta E_0}{E_0}\right) = \frac{8\pi^2}{\lambda_0^2}\left(\frac{\delta f}{f_0}\right)$$

where df/fo is the local variation in resonant frequency
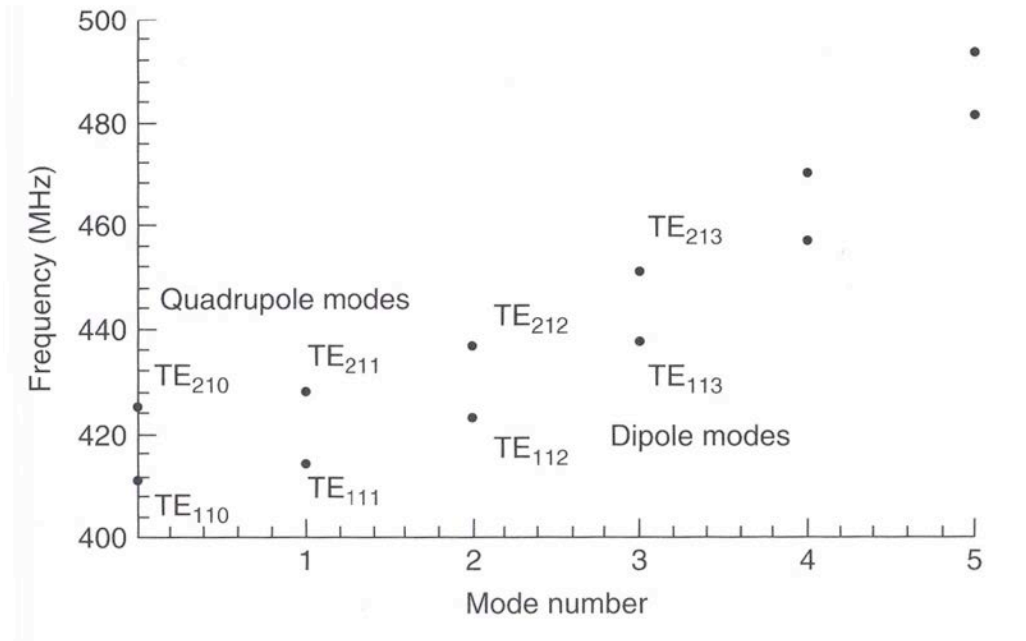
Various 4-vanes RFQ modes.

(a) Quadrupole and (b,c) dipole RFQ modes.

Los Alamos
NATIONAL LABORATORY

Suppression of Unwanted RFQ Modes

Vane coupling rings that electrically connect opposite vanes ensuring the same vane potentials. Shifts the dipole frequencies upwards eliminating their effect.

Tuning rods that shift the dipole mode frequencies upwards. The simplest approach is rods attached to the end plates that extend into the midplane of each quadrant.

Adjustable slug tuners in all four quadrants along the outer walls. These also allow us to adjust the longitudinal vane voltage profile and compensate for nearby longitudinal modes.
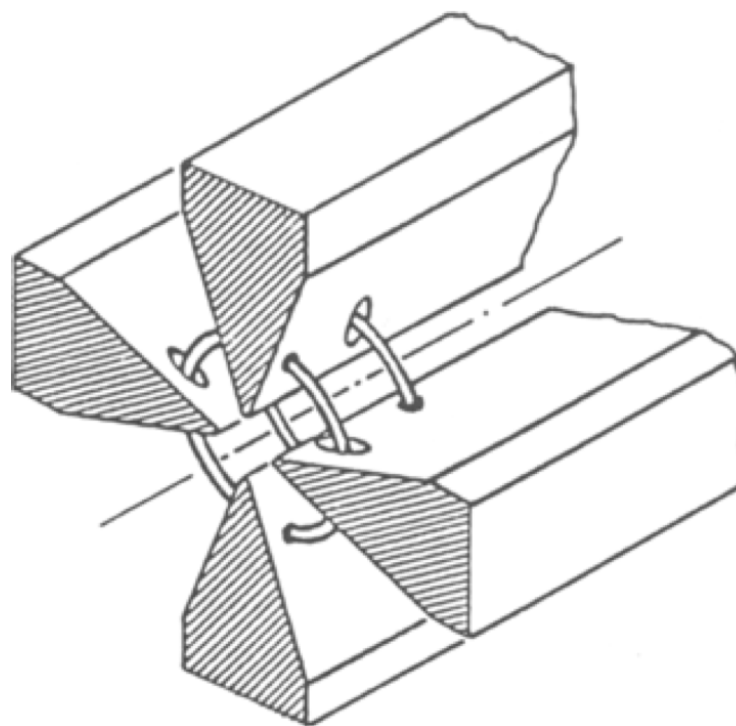
Figure 12: RFQ with Vane Coupling Rings

4-Rod RFQ Structures
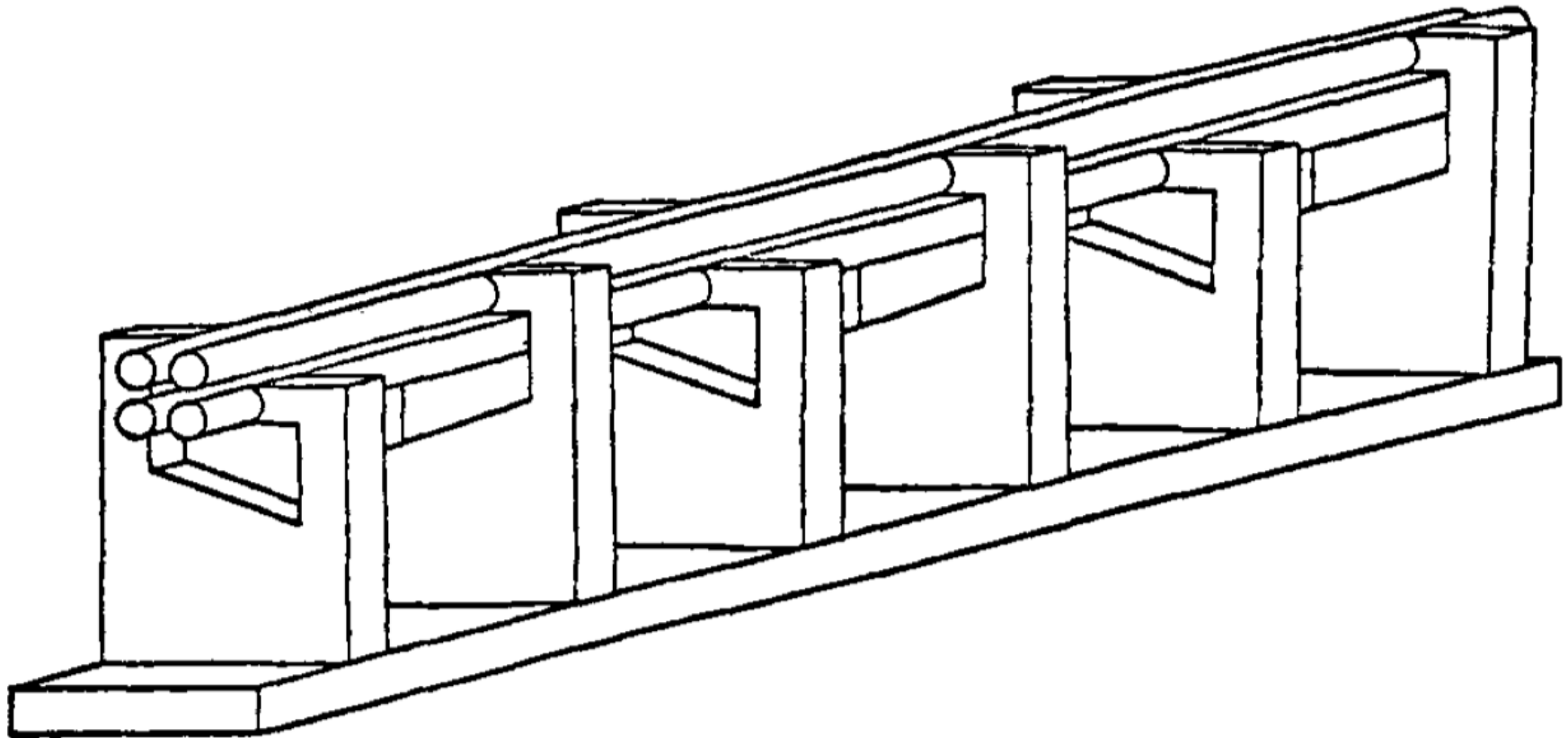
Figure 10: Four-Rod RFQ Structure

4-Rod RFQ Structures

Mode mixing is not an issue
Simple tuning
Suitable for low frequencies < 200 MHz

C_E

L

I
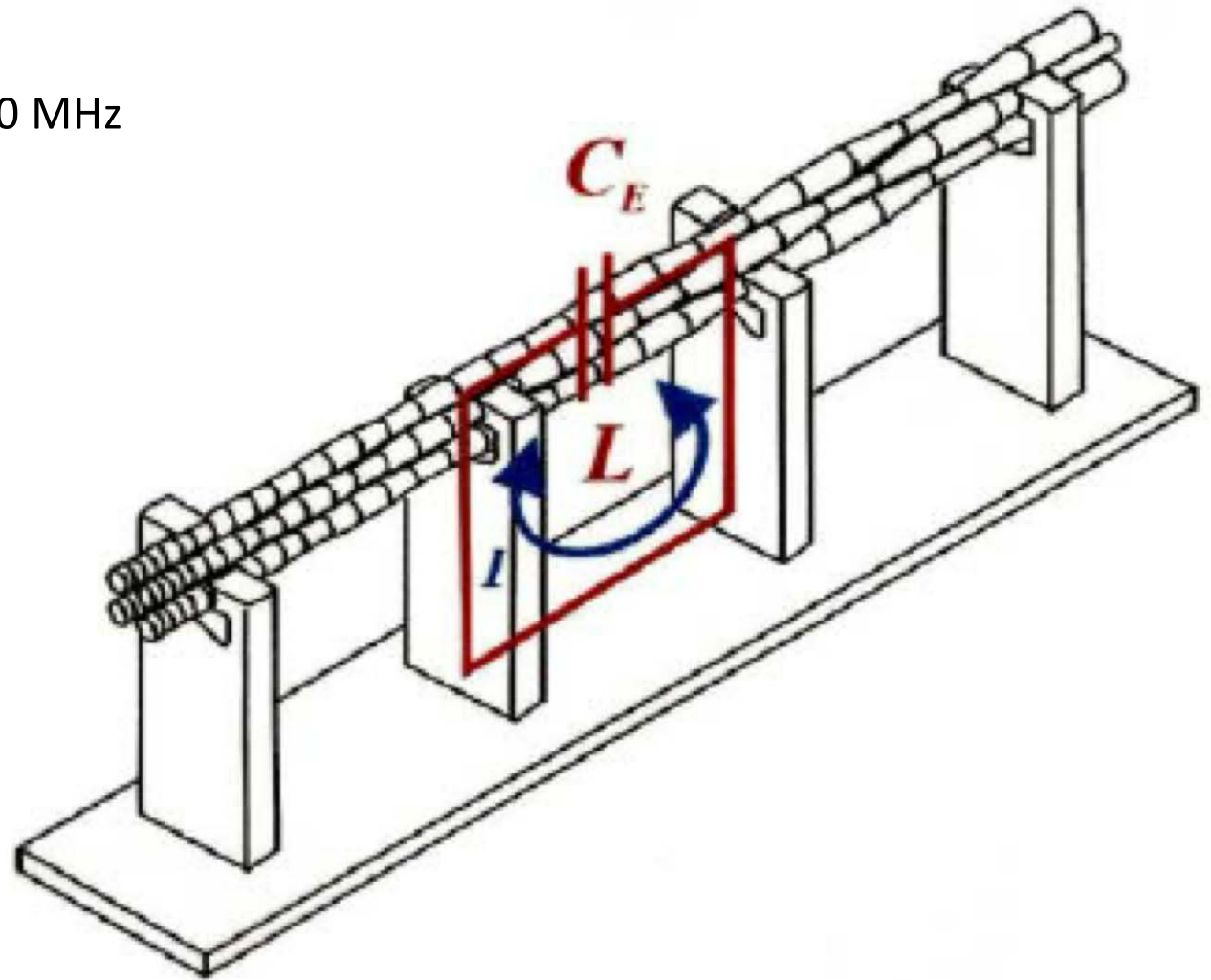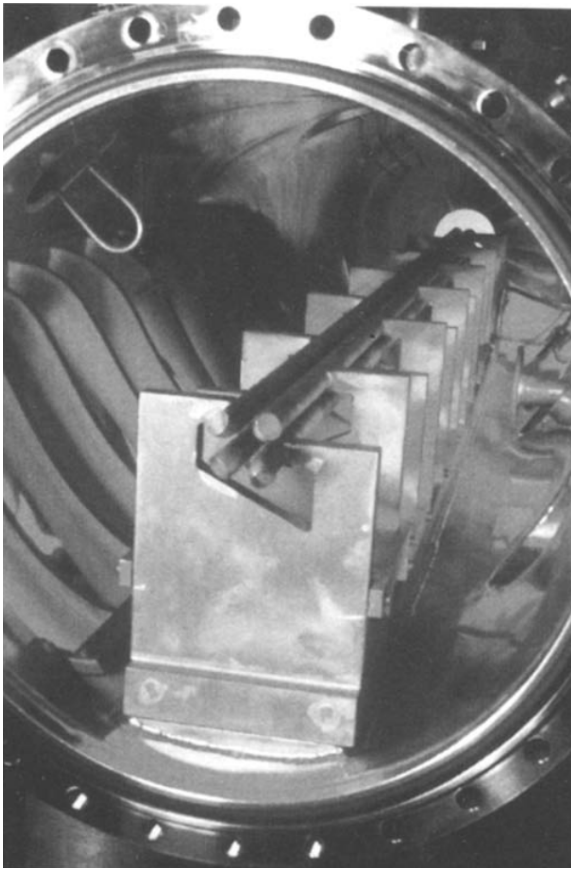
4 rod RFQ structure (A.Schempp).

Los Alamos
NATIONAL LABORATORY

Spiral 4-Rod RFQ Structure
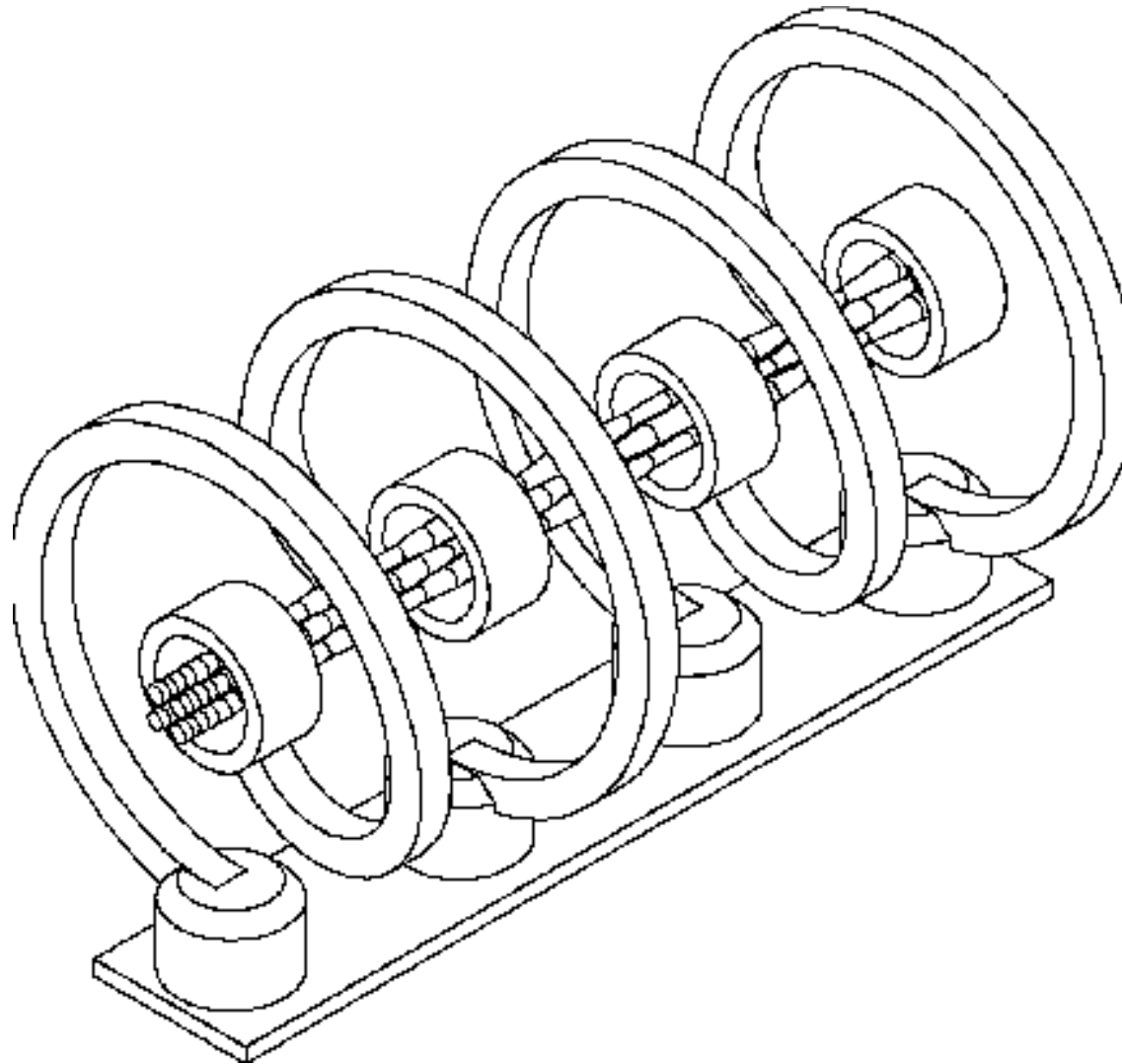
Split Coaxial RFQ Structure
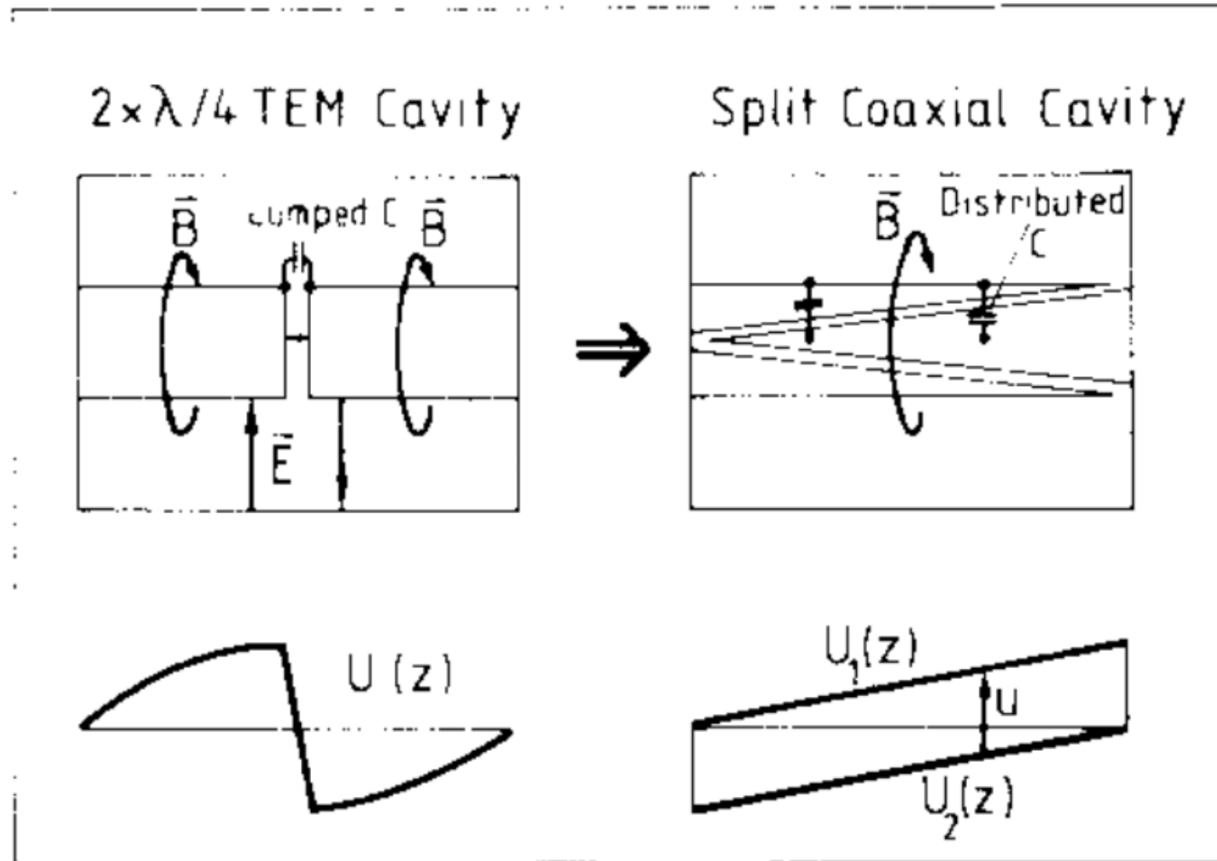
Fig. 1: Mental evolution of a 2 x λ/4 TEM cavity into an SC cavity.

Split Coaxial RFQ Structure
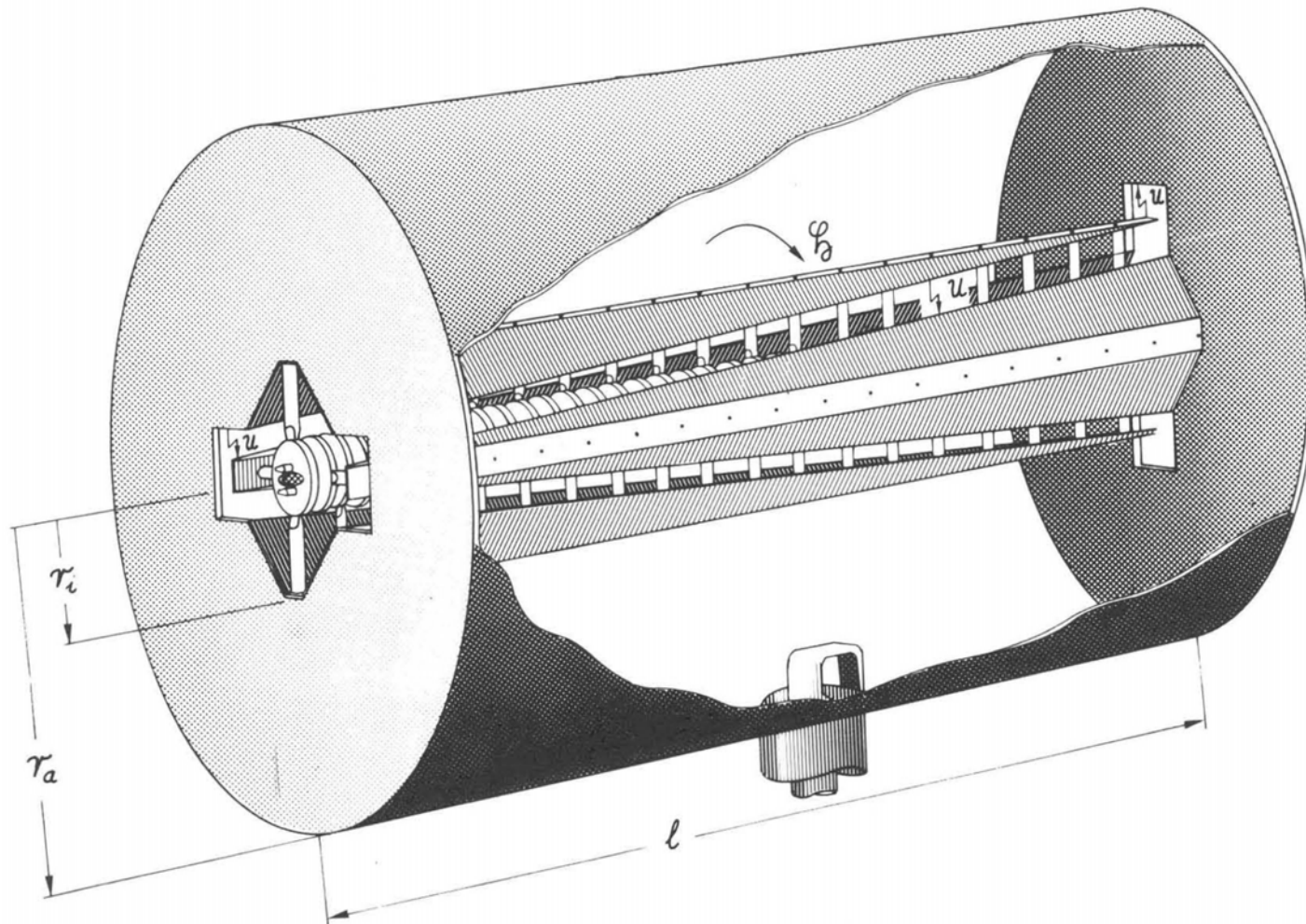
Fig. 5. Rf Cavity

Split Coaxial RFQ Structure

RF COUPLER

COUPLING RING

SPEAR-SHAPED BACK PLATE
OF VANE

VERTICAL STEM

STEM FLANGE

HORIZONTAL STEM

VERTICAL VANE

HORIZONTAL VANE
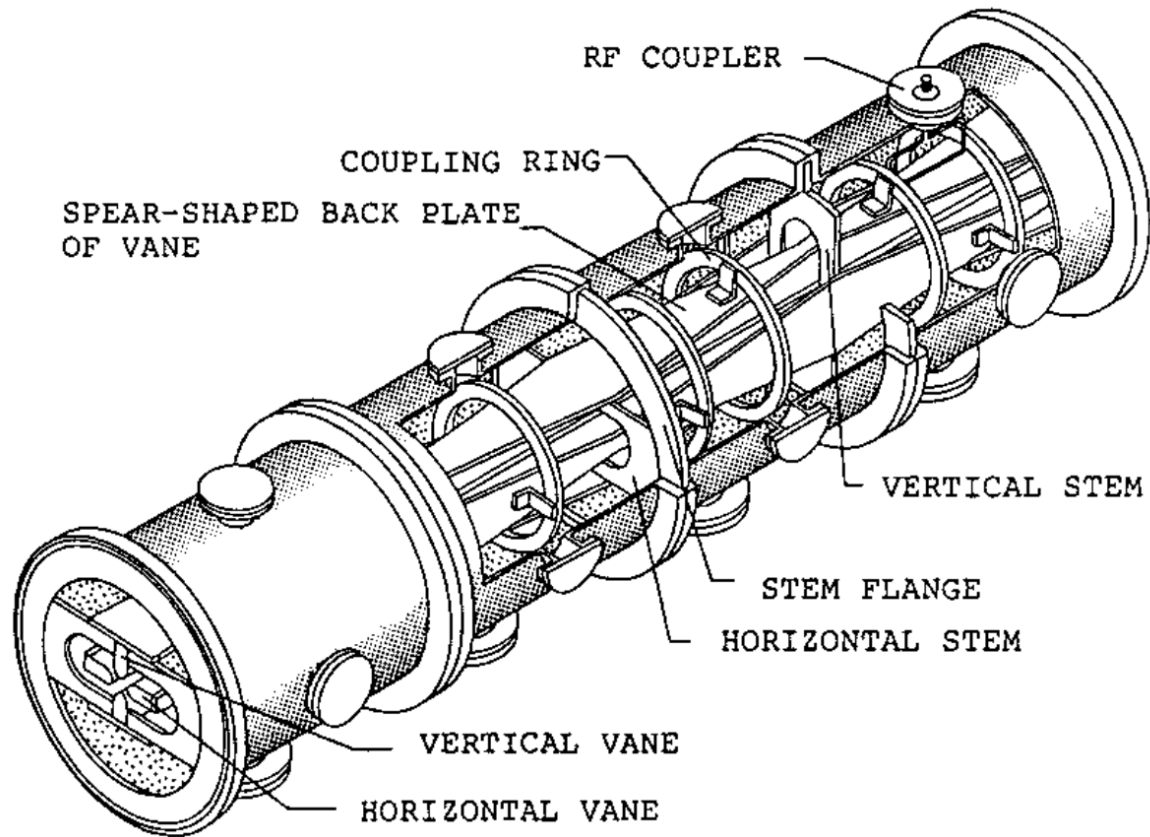
Fig. 1 Structure of the four-vane SCRFQ.

Split coaxial RFQ at INS

Los Alamos
NATIONAL LABORATORY

Shunt impedance of RFQ Structures
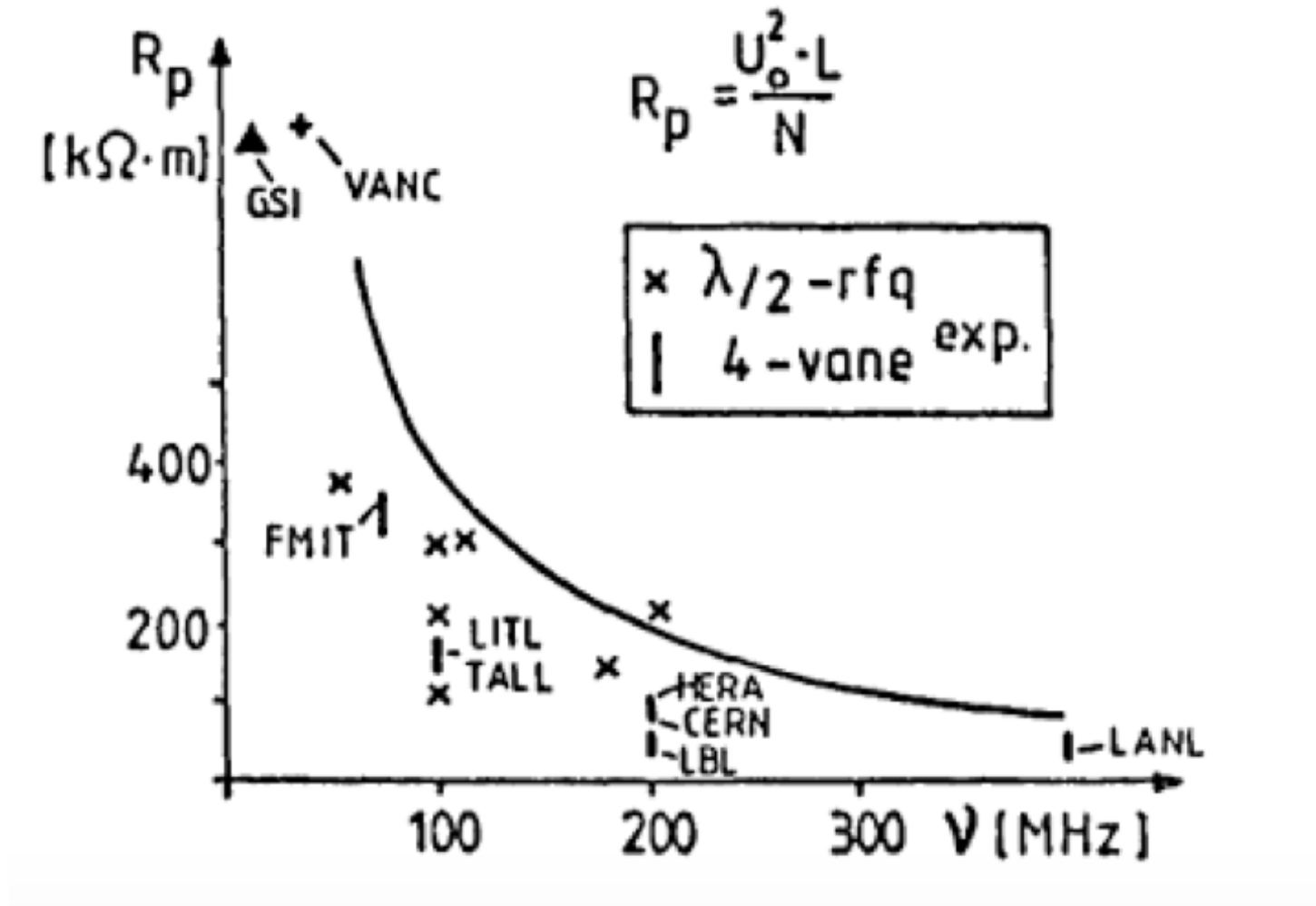
4-Rod LANL RFQ for LANSCE Upgrade (2015)
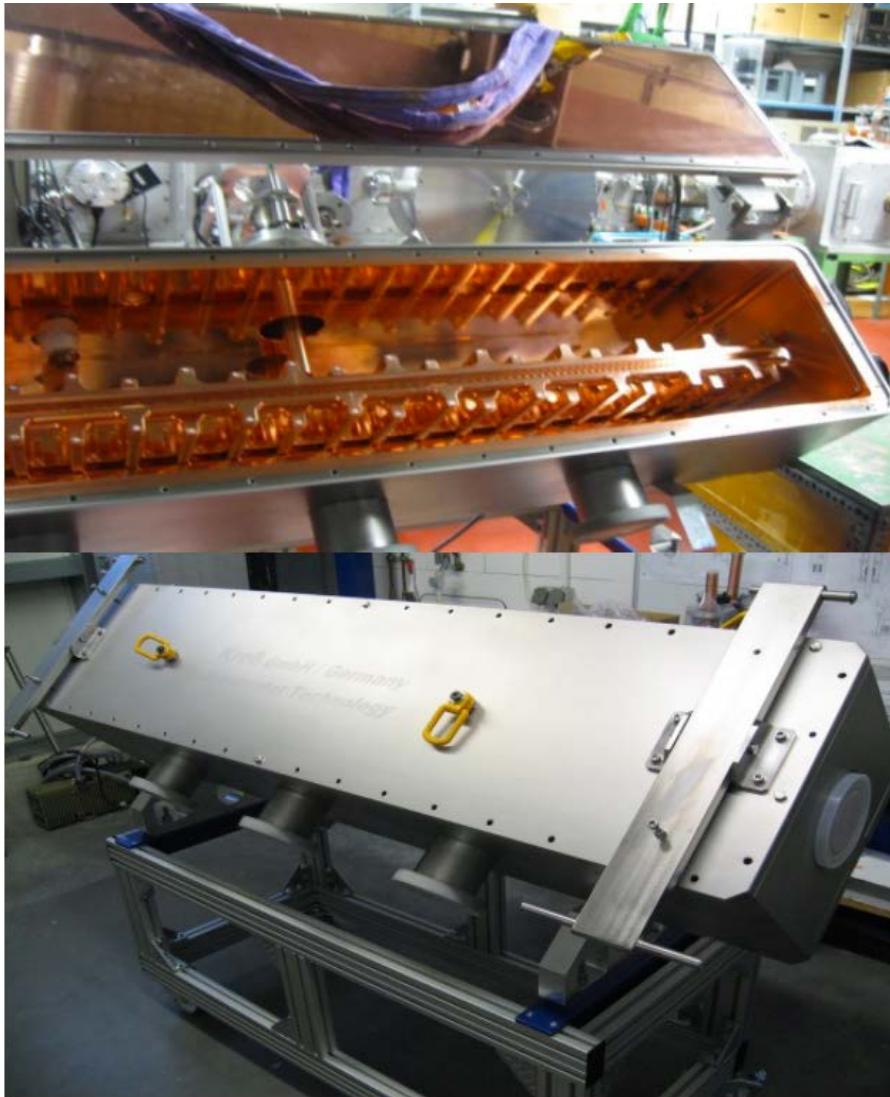
- Resonance frequency: 201.25 MHz
- Particle energy: 35 – 750 MeV/u
- Electrode voltage: 50 kV
- Length: 2000 mm
- Cross section: 400 x 420 mm

RFQ by Kress, GmbH (Germany) for proton beam upgrade at LANL.

Four-Vane with Windows RFQ

P.Ostroumov, A.Kolomiets, PRSTAB (2002)
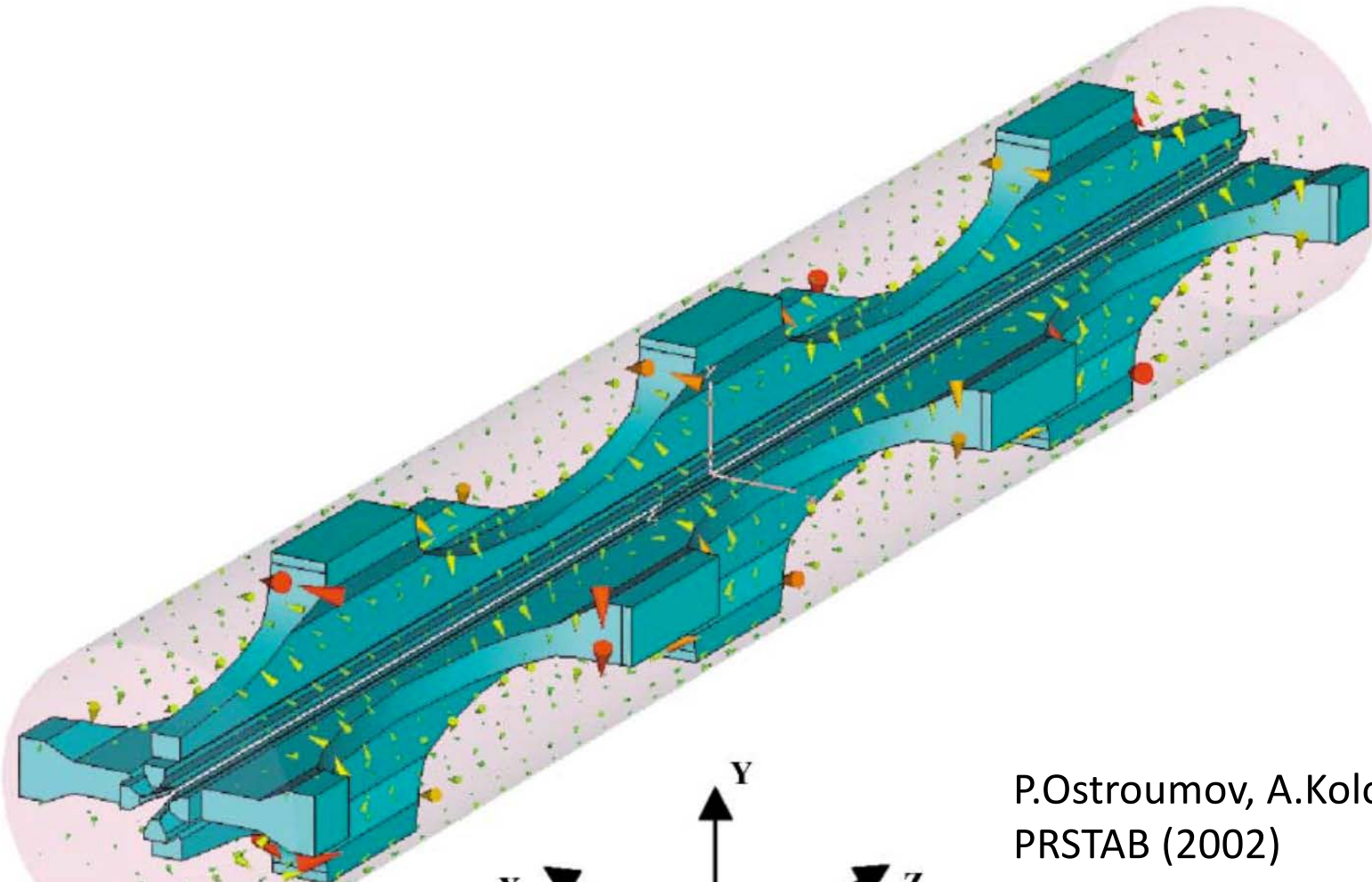
Type   = H-Field_(peak)
Monitor   = Mode 1
Maximum   = 16204.2 A/m
Max. Arrow = 5015.06 A/m
Frequency   = 57.6829
Phase   = 90 degrees

0   5.02e+003 A/m

Los Alamos
NATIONAL LABORATORY

Four-Vane with Windows RFQ (cont.)

Figure 2: view of the RFQ with open outlet flange
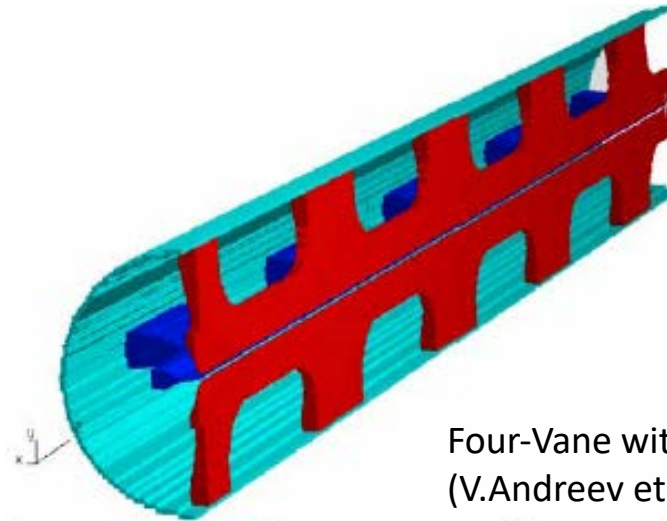
Four-Vane with Windows RFQ
(V.Andreev et al, IPAC2011)

Layout of the ½ resonator without end flanges.

Table 1: Main parameters of the RFQ structure

Parameter	Unit	Value
Operating frequency	MHz	81.5
Charge to mass ratio		1/3
Input/output energy	MeV/u	0.02/1.57
Average radius	mm	10
Vane tip radius	mm	7.5
Voltage	kV	182.5
Input emittance (norm)	cm*mrad	0.327
Output emittance (effective)	mm*mrad	2.3*π
Input current	mA	100
Pulse repetition	Hz	1
Pulse duration	μs	100
Output energy spread	keV/u	+/- 20
Length of the RFQ vanes	m	6.258
Inner cavity diameter	m	0.564
Quality factor of the resonator		11000

Los Alamos
NATIONAL LABORATORY

Parameters of Various RFQs (A.Pisent, PAC09)

Table 1: General Parameters of Various RFQs (→ means "non operated")

RFQ (design by...)		Ion (A/q)	Final energy	Vane voltage	Beam current	Beam power	RF power	Freq.	Length		Emax	Av. Power density	Max. Power density
			MeV/u	kV	mA	kW		MHz	m	λ	kilp.	W/cm²	
	→ IFMIF EVEDA (LNL)	d	2.5	79-132	130	650	585	175	9.8	5.7	1.8	3.5	30
pulsed	CERN linac 2 (CERN)	p	0.75	178	200	150	440	202	1.8	1.2	2.5	-	-
pulsed	SNS (LBNL)	H-	2.5	83	70	175	664	402.5	3.7	5.0	1.85	11.4	10
pulsed	CERN linac 3 (LNL)	8.3	0.25	70	0.08	0.04	300	101	2.5	0.8	1.9	-	-
CW high p	LEDA (LANL)	p	6.7	67-117	100	670	1450	350	8	9.3	1.8	11.4	65
CW high p	FMIT (LANL)	d	1	185	100	193	407	80	4	1	1	-	-
CW high p	→ IPHI (CEA)	p	3	87-123	100	300	750	352	6	7.0	1.7	15	120
CW high p	→ TRASCO (LNL)	p	5	68	30	150	847	352	7.3	8.6	1.8	6.6	90
CW med. p	→ SARAF (NTG)	d	1.5	65	4	12	250	176	3.8	2.2	1.4	24	54
CW med. p	→ SPIRAL2 (CEA)	3	0.75	100-113	5	7.5	170	88	5	1.5	1.65	0.6	19
CW low p	ISAC (TRIUMF)	30	0.15	74	0	0	150	35	8	0.9	1.15	-	-
CW low p	PIAVE (LNL)	7.3	0.58	280	0	0	8e-3 (SC)	80	2	0.5	2.1	-	-

Parameters of Heavy Ion RFQs (A.Schempp, 1993)

Table II: Performance of heavy ion ion RFQs

	Ion	Energy [MeV/u]	Frequency [MHz]	Length [m]	Beam current [mA]	Duty factor [%]	Impedance [kΩm]
LBL LI	S^{4+}	0.2	200	2.25	0.1	0.2	27
LNS SATURNE	Ne^{5+}	0.183	200	2.3		0.025	25
INS TALL	Li	0.8	100	7.25		10	95
CERN HI	O^{6+}	0.14	202.5	0.86		0.03	27
MSI CRYRING	Ne^{+}	0.3	108.5	1.55		0.1	110
GSI HLI	U^{28+}	0.3	108.5	2.85		25	110
GSI MAXILAC	Kr^{+}	0.045	13.1	9.4	5	5	400
ITEP HI	Xe^{2+}	0.036	6.1	12	10	1	145
INS SCR	Xe^{4+}	0.045	25.5	2.1	2.5	10	190
GSI HCI-P	U	0.0175	27.15	4.0	25	1	300
CERN Pb	Pb^{25+}	0.25	101.25	2.5		0.03	100
IPNL Cluster	$M50^{+}$	0.05–.1	85–115	2		25	100
IKF VE	Xe^{21+}	0.1–02	80–110	1.45		25	100
GSI HCI-P	U^{2+}	0.02	27.15	4.0	25	1	300

36 MHz - HIS- RFQ at GSI

First Module

Girder Undercut

Beam

925

925

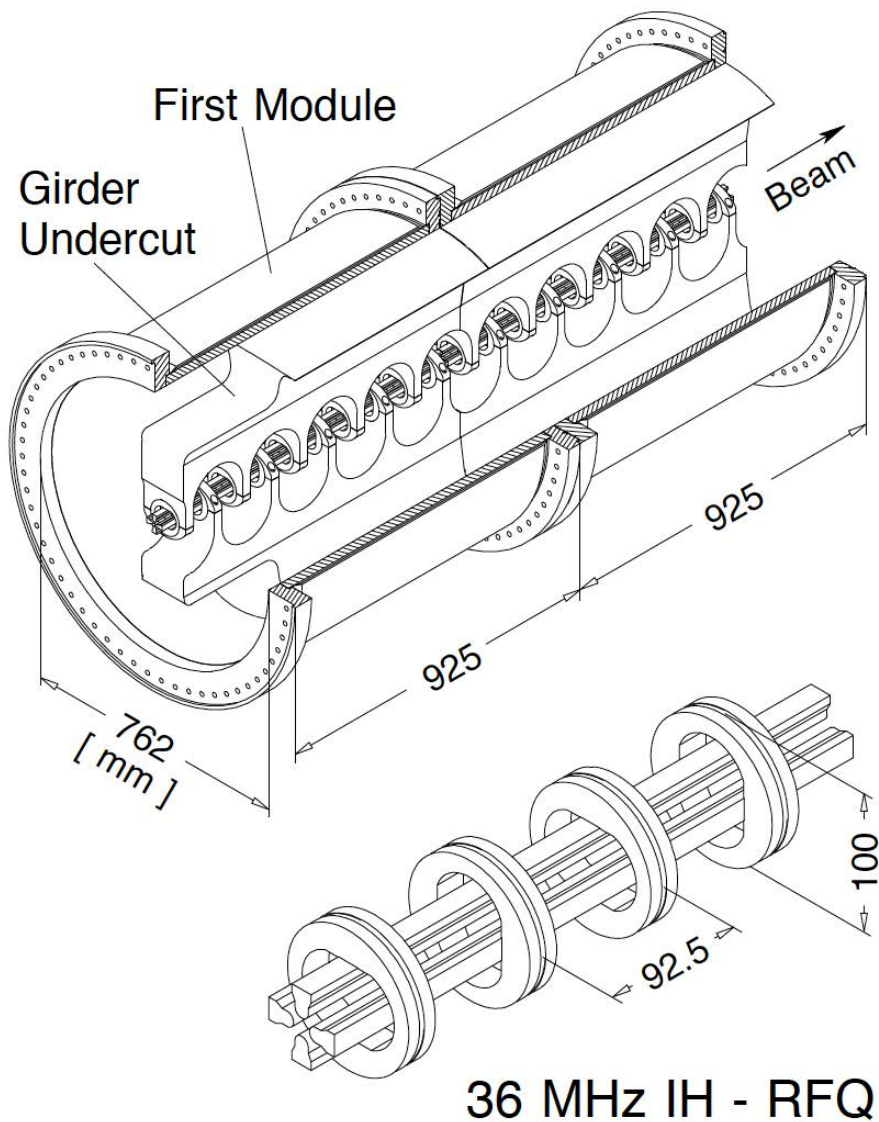762 [mm]

100

92.5

36 MHz IH - RFQ

Fig. 4. First two modules of the IH-RFQ and enlarged illustration of the electrode structure with carrier rings.

injection energy / keV/u	2.2
exit energy / keV/u	120
total length / m	9.2
resonance frequency / MHz	36.136
inner diameter / m	0.762
shunt impedance / kΩm	~ 600
Q-value	~10000
electrode voltage / kV at A/q = 65	137
min. aperture diameter / mm	7.6
min. van-vane distance / mm	4.9
ρ/R_o	0.85
needed duty factors:	
for beams with A/q ≤ 65	1 %, 10 Hz
for beams with A/q ≤ 24	30 %, 50 Hz
distribution of heat losses / %:	
mini-vanes	4
stems with carrier rings	24
ridges	24
tank wall	48

27 MHz ITEP Heavy Ion RFQ

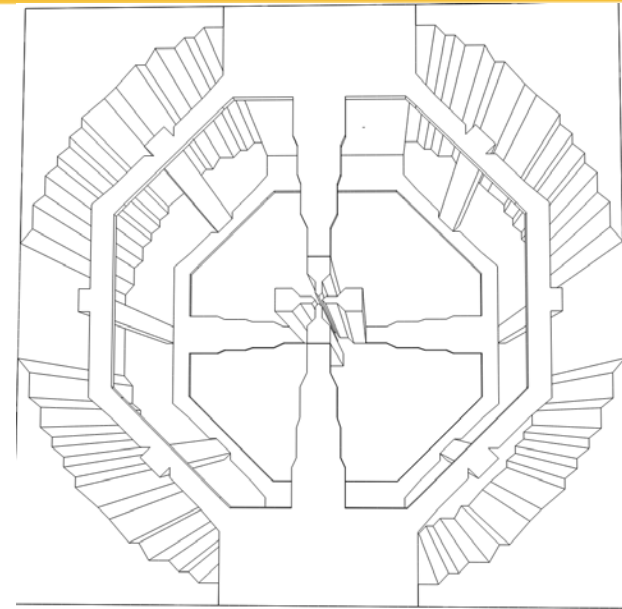|	
Length of the vacuum tank	12.0 m
Inner tank diameter	1.2 m
Outer diameter of the rings	0.81 m
Aperture radius	0.64 cm
Peak E-field on the electrode surface	2.2 Kilpatric
Transmission at 15 mA	96 %
Specific shunt-impedance (R_{sh})	1.49 MΩ·m
Emittance	0.3 mm·mrad

Table 2: Calculated and measured RF parameters

	Calculated	Measured
Frequency of quadrupole mode, MHz	27.14	27.66
Q-factor	13000	5650
Frequency of dipole mode, MHz	37.2	36
Shunt-impedance, MOhm * m	1.1	0.48

Figure 1: View of the RFQ structure at the assembling place.

Los Alamos
NATIONAL LABORATORY

35 MHz ISAC Heavy Ion RFQ at TRIUMF

RF Structure   4-rod split ring, no shaper and buncher
Ions A/Z   30
Frequency   35 MHz
Length   8 m (instead of 12 m with shaper and buncher)
Input energy   2 keV/u
Output energy   150 keV/u
Synchronous phase   -25°
Intervane voltage   75 kV
Modulation   2.6
Aperture   0.74 - 0.37 cm
RF power   75 kW

Table 1: Basic Parameters of the REX/HIE-ISOLDE RFQ

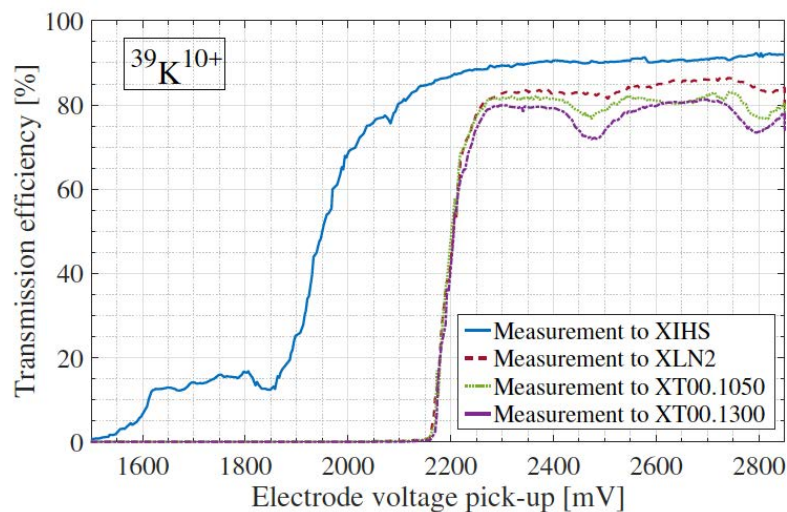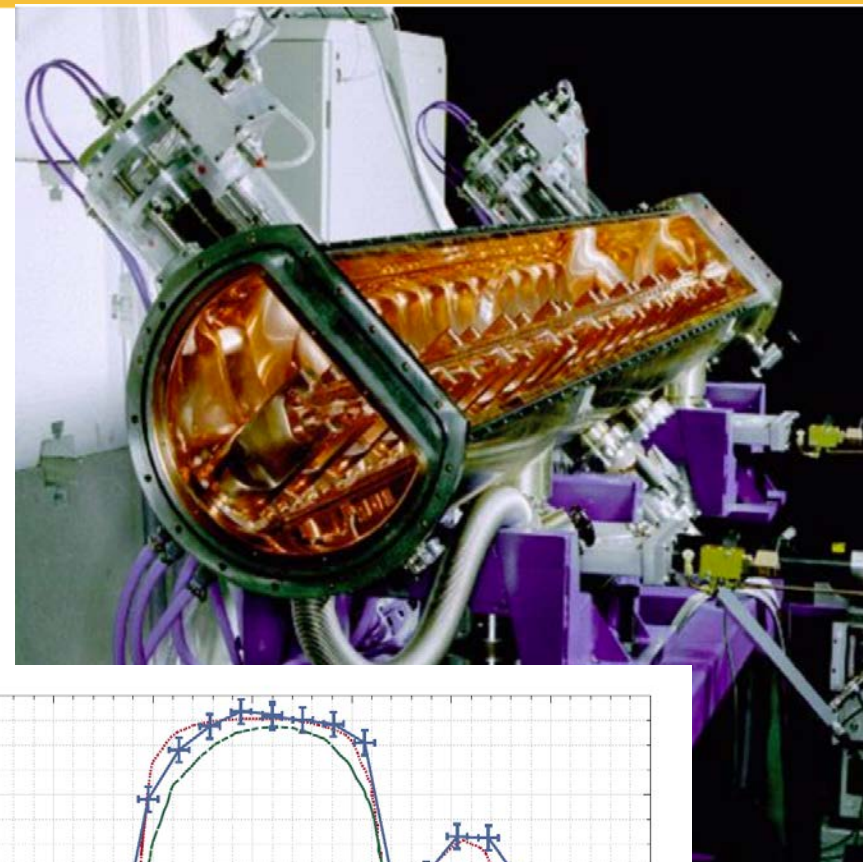| Parameter	Value
Frequency	101.28 MHz
Number of cells	232
Input energy	5 keV/u
Final energy	300 keV/u
Maximum duty cycle	10 %
A/q-acceptance	< 5.5
Radial acceptance ϵ^{norm}	$0.66\,\pi$ mm mrad
Electrode voltage ($A/q = 4.5$)	42 kV
RF Power ($A/q = 4.5$)	36.3 kW
Quality factor Q_0	3801 [2]

Figure 2: Transmission through the RFQ for $^{39}K^{10+}$ beam, measured in different locations with Faraday cups.
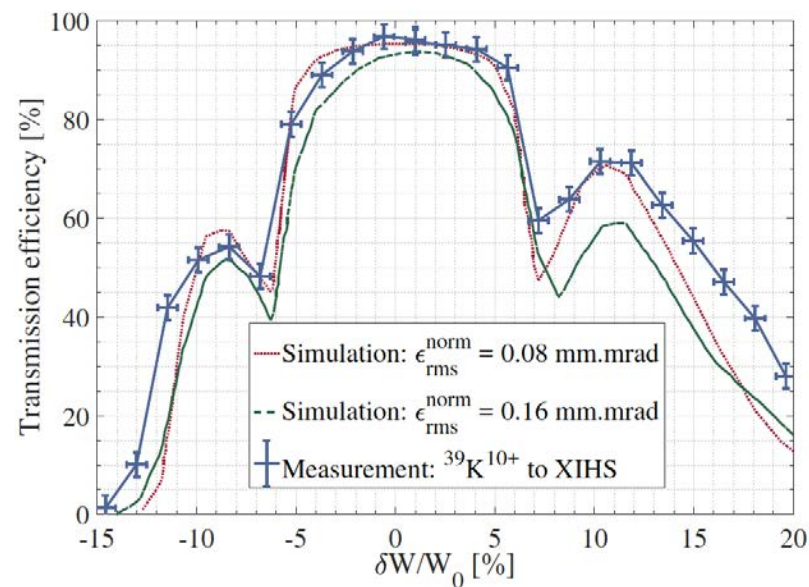
Figure 4: Measurement of the RFQ longitudinal acceptance and simulations for different transverse emittances [5].
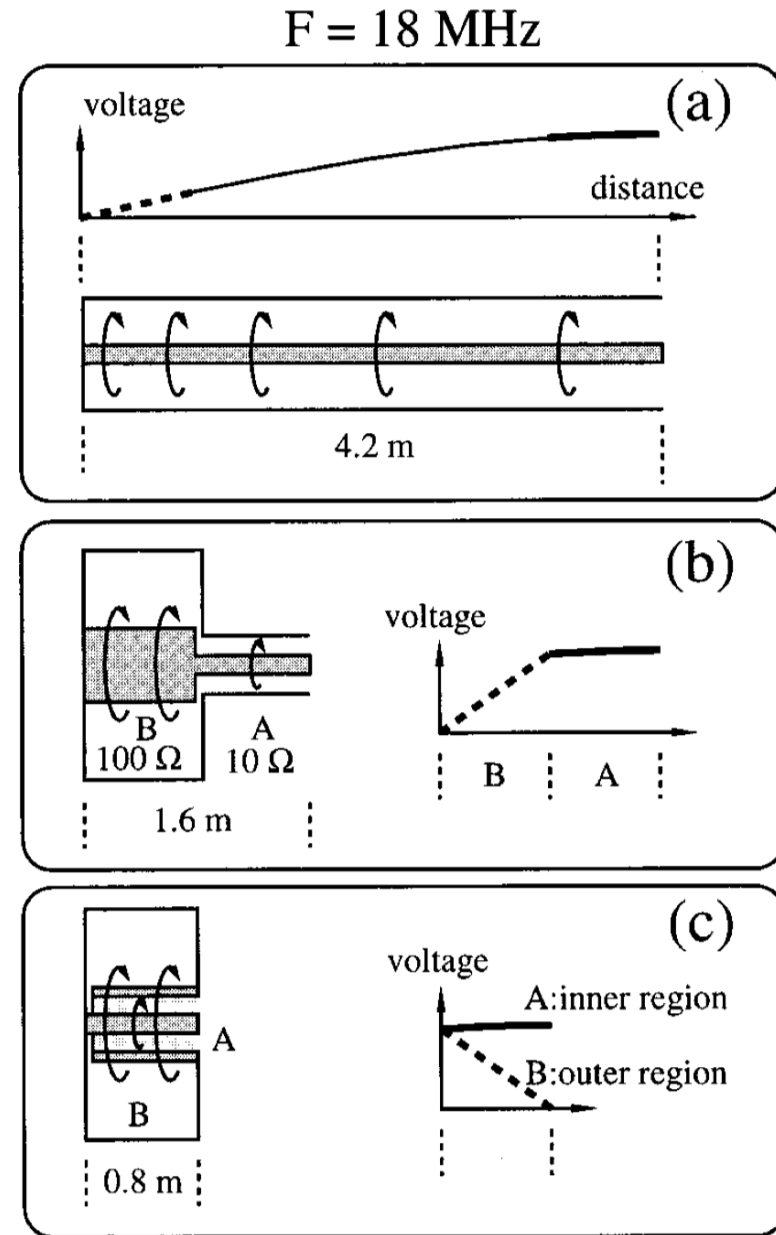
RIKEN Variable Frequency Heavy - Ion RFQ

Various types of quarter-wavelength coaxial resonator with the respective voltage distribution.

a) Straight coaxial resonator of constant characteristic impedance. The length is 4.2 m at the resonant frequency of 18 MHz.

b) Deformed coaxial resonator. If the characteristic impedance of the open-end side and that of short-end side are chosen to be 10 and 100 V, respectively, the length can be made 1.6 m at the same frequency.

 c) Folded-coaxial resonator. Now the length can be made one fifth compared with the straight resonator. The voltage distribution is almost flat in the inner region (A) of the tube.

(O. Kamigaito et al, 1999)

F = 18 MHz

Los Alamos
NATIONAL LABORATORY
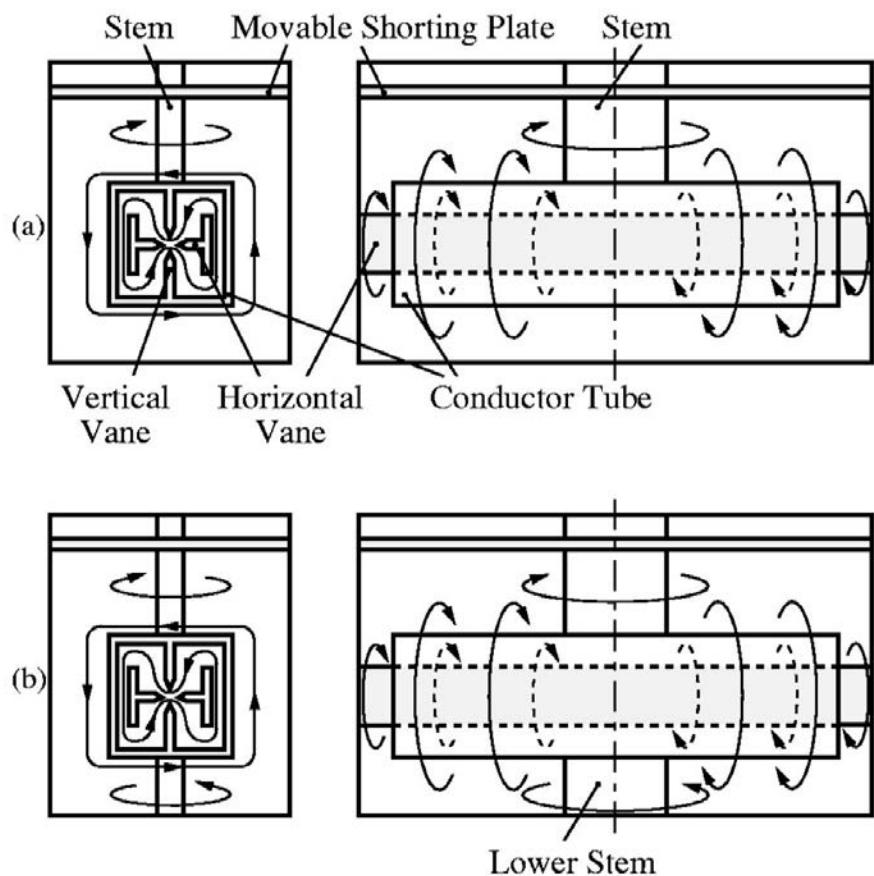
RIKEN Variable Frequency Heavy - Ion RFQ

FIG. 3. Magnetic flux of the fundamental mode of the proposed folded-coaxial RFQ. (a) Low-frequency operation without the lower stem. (b) High-frequency operation with the lower stem.
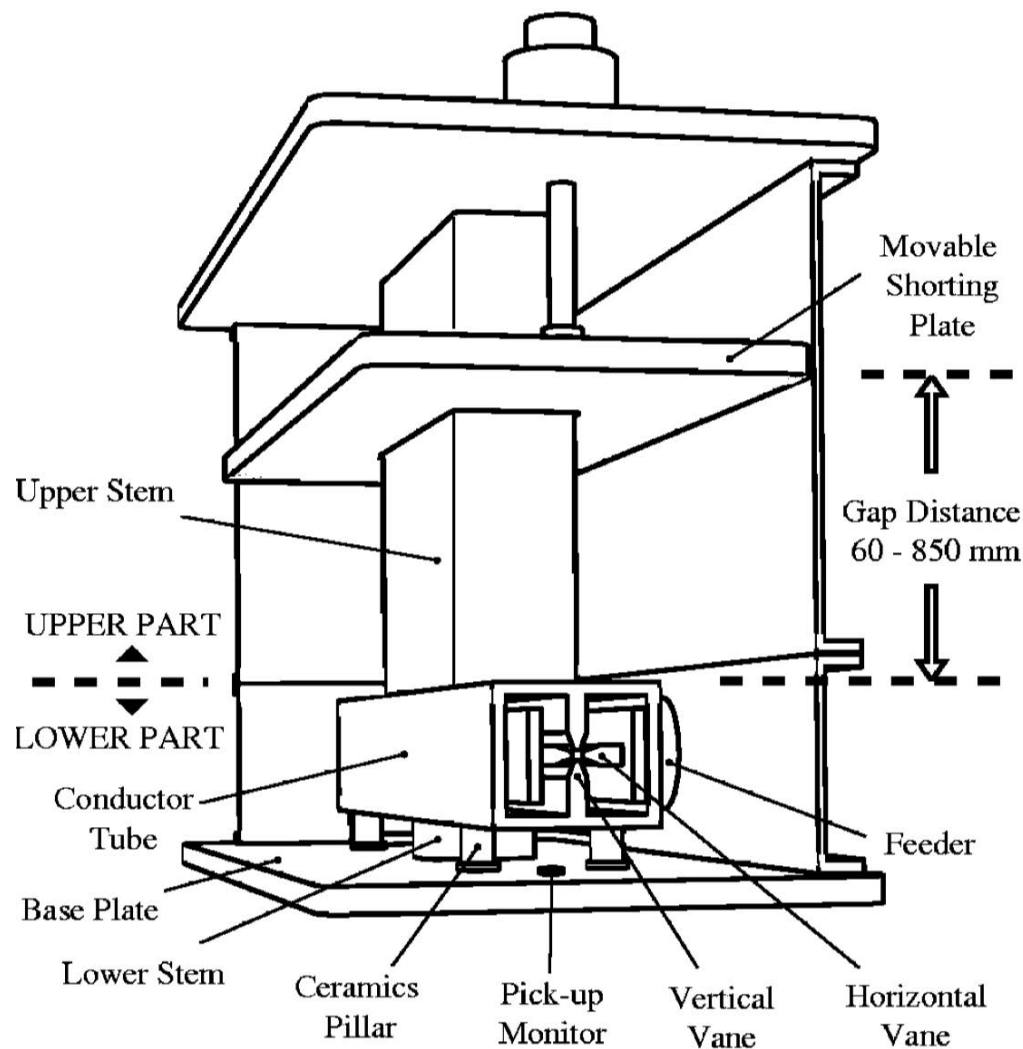

FIG. 4. Schematic drawing of the folded-coaxial RFQ resonator.

RIKEN Variable Frequency Heavy - Ion RFQ

TABLE I. Main parameters of the RFQ.

	To July 1997	From August 1997
Frequency (MHz)	17.7–39.2	17.4–39.0
Duty	100%	100%
Mass-to-charge ratio (m/q)	25.5–5.2	26.4–5.3
Input energy (keV/q)	10	20
Output energy (keV/q)	450	450
Input emittance (mm mrad)	145π	145π
Vane length (cm)	142	153
Intervane voltage (kV)	33.6	36.8
Mean aperture (r_0:mm)	7.70	8.08
Min. aperture (a:mm)	4.17	4.67
Max. modulation (m)	2.70	2.41
Beam margin	1.7	1.6
Focusing strength (B)	6.8	6.8
Max. defocusing strength (Δ_{rf})	−0.3	−0.3
Final synchronous phase	−25°	−30°

Los Alamos
NATIONAL LABORATORY
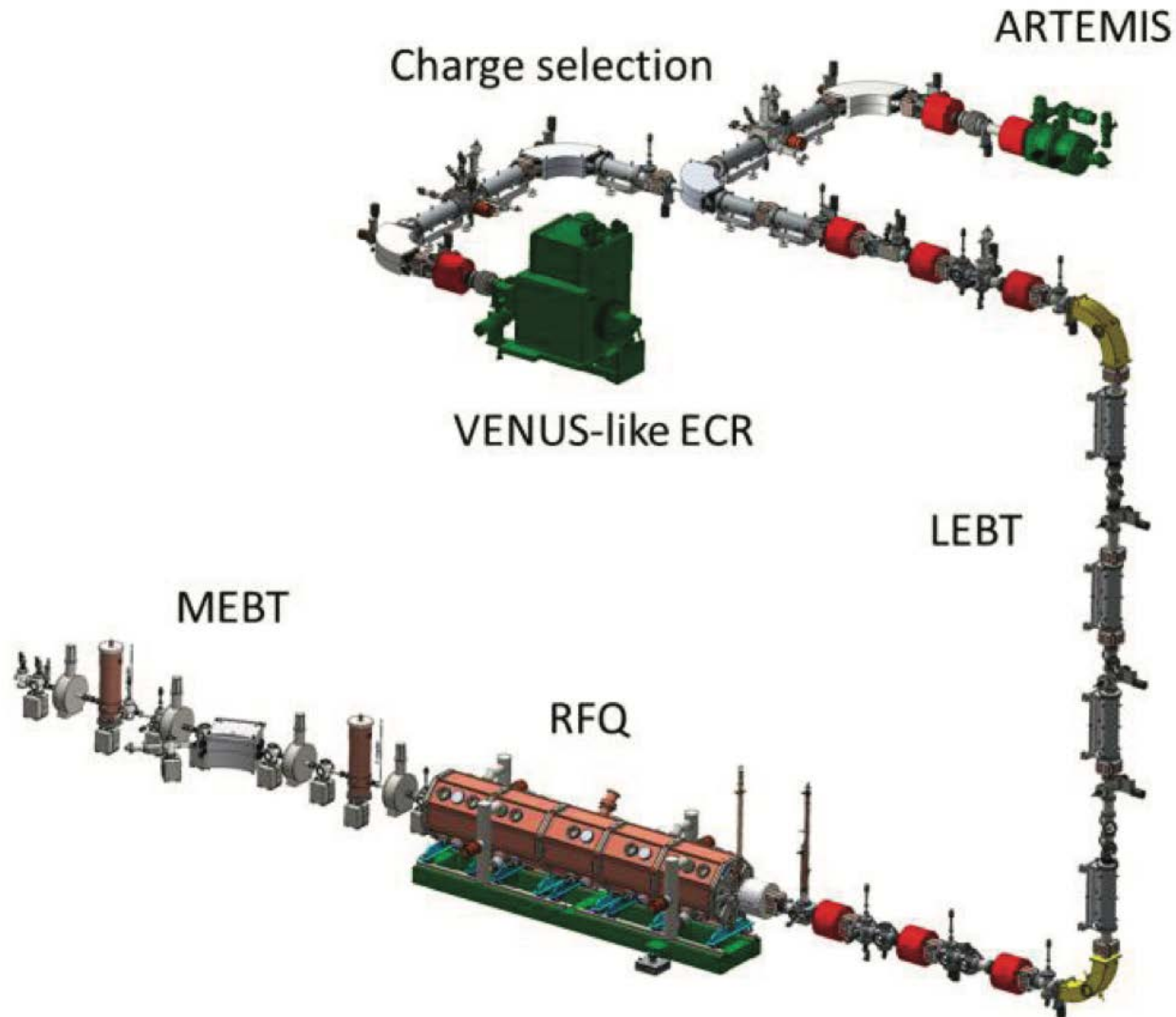
FRIB MSU Front End

FRIB Front End Layout. Two ECR sources are located at the ground level. The RFQ and MEBT are located in the linac tunnel 10 m below grade.

FRIB MSU RFQ

FRIB RFQ Design Parameters

Frequency (MHz)	80.5
Injection/Output energy (keV/u)	12/500
Beam current (typical, μA)	450
Beam emittance (full, norm, πμm)	1.0
Long. Emittance (99.9%, keV/u-ns)	1.5
Transmission efficiency (typical, %)	80
Design charge-to-mass ratio	1/7-1/3
Accelerating voltage ramp (U, kV)	60 – 112
Surface electric field (Kilpatrick)	1.6
Quality factor	16500
Operational RF power (kW, O-U)	15 – 100
Length (m)	5.04

FRIB RFQ full assembly model and segment 1 assembly (Bultman et al, IPAC2013)

Los Alamos
NATIONAL LABORATORY
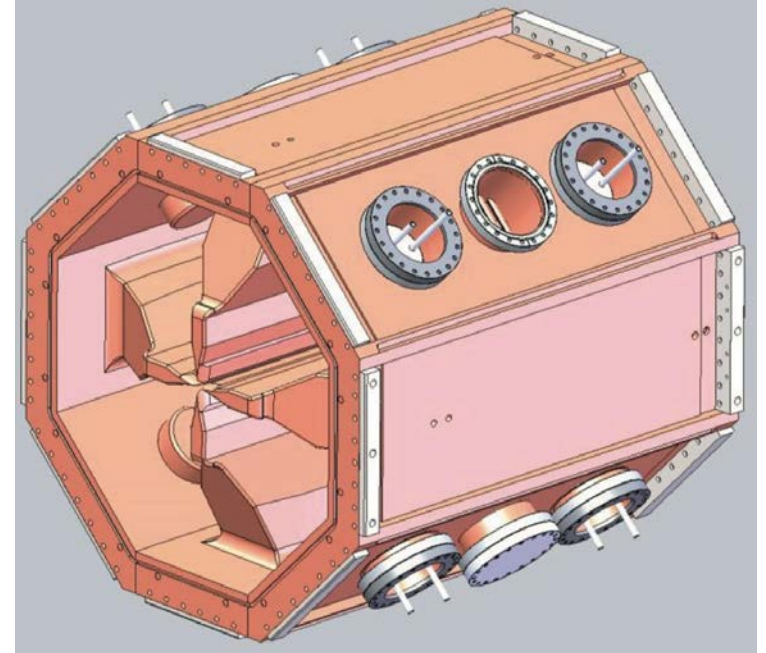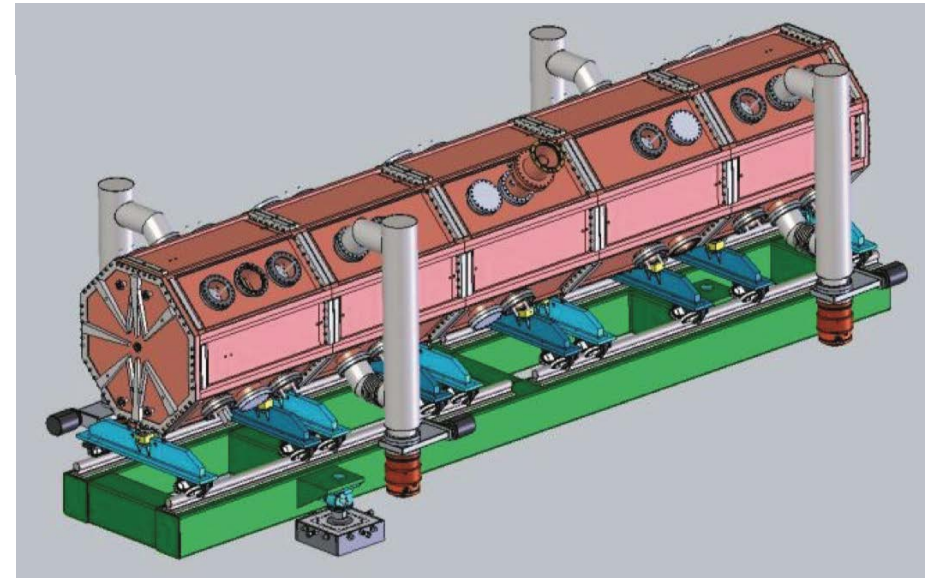
Conclusions

1. RFQ provides acceleration and focusing by the same electric field.

2. The use of electric field rather than magnetic field provides strong focusing for low-energy particles.

3. RFQ accelerator does not require high-voltage injector.

4. RFQ has large acceptance, high capture efficiency, high peak current, small emittance growth.

5. RFQ accelerating gradient drops with energy. RFQ is effective as an initial part of high-intensity accelerator up to energy of 3-5 Mev per nucleon.

6. Heavy-ion RFQ requires RF frequency within the range of 18 – 35 MHz. Expected length of heavy-ion RFQ is within 8 -13 m. Inclusion of multi-harmonic buncher is an option to reduce the length of RF structure.